British Geological Survey
NATURAL ENVIRONMENT RESEARCH COUNCIL

Microbial Impacts of CO_2 transport in Sherwood Sandstone

Minerals and Waste/Energy Programme
Open Report OR/12/023

BRITISH GEOLOGICAL SURVEY

MINERALS and Waste/Energy PROGRAMME

OPEN REPORT OR/12/023

Microbial Impacts of CO_2 transport in Sherwood Sandstone

J Wragg, J Rushton, K Bateman, K Green, H Harrison, D Wagner, A E Milodowski and J M West

Keywords

CCS, microbes**,** sandstone.

Front cover

ESEM of post-test sandstone sample highlighting a quartz overgrowth and patchy film like deposits.

Bibliographical reference

WRAGG, J, RUSHTON, J, BATEMAN, K, Green, K, Harrison, H, Wagner, D, Milodowski, A E and West J M . 2013. All fields on the title and cover should be amended by using File/Properties/Custom. *British Geological Survey Open Report*, OR/12/023. 60pp.

Keyworth, Nottingham British Geological Survey 2013

BRITISH GEOLOGICAL SURVEY

The full range of our publications is available from BGS shops at Nottingham, Edinburgh, London and Cardiff (Welsh publications only) see contact details below or shop online at www.geologyshop.com

The London Information Office also maintains a reference collection of BGS publications, including maps, for consultation.

We publish an annual catalogue of our maps and other publications; this catalogue is available online or from any of the BGS shops.

The British Geological Survey carries out the geological survey of Great Britain and Northern Ireland (the latter as an agency service for the government of Northern Ireland), and of the surrounding continental shelf, as well as basic research projects. It also undertakes programmes of technical aid in geology in developing countries.

The British Geological Survey is a component body of the Natural Environment Research Council.

British Geological Survey offices

BGS Central Enquiries Desk

Tel 0115 936 3143 Fax 0115 936 3276

email enquires@bgs.ac.uk

Kingsley Dunham Centre, Keyworth, Nottingham NG12 5GG

Tel 0115 936 3241 Fax 0115 936 3488

email sales@bgs.ac.uk

Murchison House, West Mains Road, Edinburgh EH9 3LA

Tel 0131 667 1000 Fax 0131 668 2683

email scotsales@bgs.ac.uk

London Information Office at the Natural History Museum (Earth Galleries), Exhibition Road, South Kensington, London SW7 2DE

Tel 020 7589 4090 Fax 020 7584 8270

Tel 020 7942 5344/45 email bgslondon@bgs.ac.uk

Columbus House, Greenmeadow Springs, Tongwynlais, Cardiff CF15 7NE

Tel 029 2052 1962 Fax 029 2052 1963

Forde House, Park Five Business Centre, Harrier Way, Sowton EX2 7HU

Tel 01392 445271 Fax 01392 445371

Maclean Building, Crowmarsh Gifford, Wallingford OX10 8BB

Tel 01491 838800 Fax 01491 692345

Geological Survey of Northern Ireland, Colby House, Stranmillis Court, Belfast BT9 5BF

Tel 028 9038 8462 Fax 028 9038 8461

www.bgs.ac.uk/gsni/

Parent Body

Natural Environment Research Council, Polaris House, North Star Avenue, Swindon SN2 1EU

Tel 01793 411500 Fax 01793 411501

www.nerc.ac.uk

Website www.bgs.ac.uk

Shop online at www.geologyshop.com

Foreword

This report is the published product of a study by the British Geological Survey (BGS) opportunities fund programme to evaluate host rock interactions with a microbial community (*Pseudomonas aeruginosa*) in the presence of saline water saturated with carbon dioxide and under realistic sub-surface conditions in the context of Carbon Capture and Storage.

Acknowledgements

We would like to thank Prof Denis Peach, BGS Chief Scientist for funding this study under the BGS Opportunities Fund programme.

Contents

Foreword ..... **i**

Acknowledgements ..... **i**

Contents ..... **i**

Summary ..... **v**

1 Introduction **1**

2 Laboratory techniques **2**

2.1 Experimental overview 2

2.2 Flow-through column methodology 2

2.3 Preparation of fluids 4

2.4 Selection and preparation of intact core material 5

2.5 Bacterial culture 5

2.6 Decomissioning of experiments 5

3 Analytical techniques **7**

3.1 Characterisation of solid materials 7

3.2 Microbial analyses 10

3.3 Chemical analyses 10

4 Results **11**

4.1 Characteristics of the sandstone starting materials 11

4.2 Characteristics of the post-experimental materials 11

4.3 Petrography 13

4.4 Microbiology 25

4.5 Physical measurement results 29

4.6 Fluid Chemistry 29

5 Discussion 38
5.1 Whole Rock and Clay mineralogy 38
5.2 Petrography 38
5.3 MicrobioloGial and Physical Measurements 39
5.4 Chemical Measurements 40

6 Conclusion and recommendations 40

Appendix 1 X-ray Diffraction Traces 41

Appendix 2 Chemistry data for the control column 42

Appendix 3 Chemistry data for the biotic column 45

Glossary ..... Error! Bookmark not defined.

References 50

FIGURES

Figure 1 Schematic of column design 3

Figure 2 Schematic of pressure vessel with column containing rock core 3

Figure 3 P/T phase diagram for water in the region relevant to ESEM operation. Tw is the triple point. Source data for the sublimation and melting curves has been derived from Wagner *et al.* (1994), and for the boiling / saturation curve is *IAPWS formulation for industrial use, 1997*. Humidity curves have been calculated and superimposed on the gas portion of the diagram. 10

Figure 4 Microbial count and pH data for the control and biotic experiments. The control pH and microbial counts are shown by a black line a closed circles respectively with the biotic experiment represented by grey closed circles and line. The pH of the starting fluid in both experiments is shown by an open grey square. The number of microbes in the pump at the end of the control experiment are shown by an open black circle. The number of microbes in the inoculant for the biotic experiment are denoted by a closed grey diamond. 26

Figure 5 Overlay of recorded pressure and microbial counts in the outflow fluids from the control and biotic columns from the start of each experiment. Black lines and closed circles relate to the control experiment and grey lines and closed circles the biotic experiment. The number of microbes in the inoculant, for the biotic experiment, is denoted by a closed grey triangle. The time of inclusion of saturated CO_2 fluid inoculation are marked on plot. 29

Figure 6 Alkalinity data measured as HCO_3^- for the control and biotic experiments. Closed black and grey circles represent the control and biotic experiments respectively. The HCO_3^- concentration in both starting fluids is shown by an open black square. 31

Figure 7 Sodium data for the control and biotic experiments. Closed black and grey circles represent the control and biotic experiments respectively. The sodium concentration in both starting fluids is shown by an open black square. 32

Figure 8 Chloride data for the control and biotic experiments. Closed black and grey circles represent the control and biotic experiments respectively. The chloride concentration in both starting fluids is shown by an open black square. 32

Figure 9 NPOC data for the control and biotic experiments. Closed black and grey circles represent the control and biotic experiments respectively. The NPOC concentration in both starting fluids is shown by an open black square. 33

Figure 10 Total iron data for the control and biotic experiments. Closed black and grey circles represent the control and biotic experiments respectively. The iron concentration in both starting fluids is shown by an open black square. 33

Figure 11 Magnesium data for the control and biotic experiments. Closed black and grey circles represent the control and biotic experiments respectively. The magnesium concentration in both starting fluids is shown by an open black square. 34

Figure 12 Nickel data for the control and biotic experiments. Closed black and grey circles represent the control and biotic experiments respectively. The nickel concentration in both starting fluids is shown by an open black square. 35

Figure 13 Potassium data for the control and biotic experiments. Closed black and grey circles represent the control and biotic experiments respectively. The potassium concentration in both starting fluids is shown by an open black square. 36

Figure 14 Silicon data for the control and biotic experiments. Closed black and grey circles represent the control and biotic experiments respectively. The silicon concentration in both starting fluids is shown by an open black square. 36

Figure 15 Antimony data for the control and biotic experiments. Closed black and grey circles represent the control and biotic experiments respectively. The antimony concentration in both starting fluids is shown by an open black square. 37

Figure 16 Tungsten data for the control and biotic experiments. Closed black and grey circles represent the control and biotic experiments respectively. The tungsten concentration in both starting fluids is shown by an open black square. 37

PLATES

Plate 1 Photograph of column components prior to final assembly and insertion into pressure vessel .....……...4

Plate 2 Photograph of assembled apparatus showing pressure vessel and syringe pump……..4

Plate 3 Example of column assembly removal from pressure vessel……6

Plate 4 Control column after removal from pressure vessel and end pieces. Arrows indicate direction of fluid flow during the experiment .....……..6

Plate 5 Biotic column after removal from pressure vessel. Arrows indicate direction of fluid flow during the experiment.....……..7

Plate 6 ESEM sample holders and preparation. a: cup holder used for rock chips. b: example cup with mm scale rock chip and pool of liquid. .....……..9

Plate 7 SEM image. Post test control sample, inlet end, 95% humidity. A patchy dark film-like deposit on the pore walls, much of it here defined by quartz overgrowth, is typically associated with deposits of mobilised fines. Boxed area is the site of the following plate……...13

Plate 8 SEM image. Post test control sample, inlet end, 95% humidity. From the boxed area in the preceding image. Diagenetic features include authigenic K-feldspars and illitic clays bridging a pore throat. There are scattered oval and rounded forms about 2 µm across scattered on pore walls. .....……14

Plate 9 SEM image. Post test control sample, inlet end, 80% humidity. A quartz overgrowth is partially coated by a thin film-like phase. There are mineral fines deposited on the surface of the film.....……14

Plate 10 SEM image. Post test control sample, inlet end, 80% humidity. A quartz overgrowth is partially coated by a thin film-like phase, commonly with a fibrous form. There are widespread mineral fines deposited on the surface of the film. 15

Plate 11 SEM image. Post test control sample, from 40-50 mm beyond the inlet face, 80% humidity. Pore walls, here defined by quartz overgrowth, have a sparse and patchy film-like coating. Boxed area is the site of the following plate. 15

Plate 12 SEM image. Post test control sample, from 40-50 mm beyond the inlet face, 80% humidity. Detail of the patchy film-like coating from the boxed area in the preceding plate. Again, the film is typically associated with fines. In detail the film commonly has a fibrous aspect. 16

Plate 13 Biotic sample during decommissioning, showing the test plug contained in the apparatus. An area of grey staining is apparent at the outlet end of the plug.....17

Plate 14 Test plug and end frits after removal of the outer casing, showing the patch of grey stain on the outside at the outlet end. Bedding planes are indicated. 17

Plate 15 Outlet end of the test plug showing the extent of the grey staining.....18

Plate 16 Biotic test plug freshly fractured, showing the strongly defined bedding structures. The grey staining observed on the outside of the plug has not penetrated the plug interior.....18

Plate 17 SEM image. Post test biotic sample, central inlet end, 90% humidity. General view showing scattered patches of a film-like deposit on pore walls, several with associated silicate fines. 19

Plate 18 SEM image. Post test biotic sample, central inlet end, 90% humidity. Detail of a quartz overgrowth with a patchy film-like deposit. A fibrous phase associated with the film is also visible draped over the top of an angular fragment of silicate. This is most likely a fibre of illitic clay. 20

Plate 19 SEM image. Post test biotic sample, central inlet end, 90% humidity. This area of pore wall defined by quartz overgrowth is partially coated by film and associated fines. There are scattered rounded oval forms <3 µm across visible within the film (unlabelled arrows).....20

Plate 20 SEM image. Post test biotic sample, edge inlet end, 90% humidity. This area of pore wall has a patchy film coating that contains common rounded, oval <3 µm forms (unlabelled arrows). 21

Plate 21 SEM image. Post test biotic sample, central inlet + 40 mm, 95% humidity. Typical patchy pore lining film with associated fines on quartz (centre, right) and K-feldspar (left) overgrowth faces.....22

Plate 22 Post test biotic sample, edge inlet + 40 mm, 95% humidity. Patchy film and associated fines on a protruding apical quartz overgrowth site. Film and fines are more abundant towards the tip. There are scattered rounded, oval <3 µm forms (unlabelled arrows). 22

Plate 23 Post test biotic sample, edge outlet, 90% humidity. Pore-lining film is sparsely distributed at the outlet end of the sample both the edge sites (as shown here) and at central sites. 23

Plate 24 Post test biotic sample, central outlet, 90% humidity. Dark areas here are residual fluids on rougher pore walls and fibrous forms laid across a partially developed quartz overgrowth. These are illitic clay forms that are laid across the overgrowth surfaces; this probable collapse could have occurred prior to, during or after the testing. 24

Plate 25 Post test biotic sample, edge outlet, 95% humidity. An example of a fibrous illitic clay cluster that has not collapsed. There is no evidence of film amongst the fibres.....24

Plate 26 SEM image. Post test biotic sample, outlet end, grey stained area, 95% humidity. A sample portion prepared from the outer grey stained surface. There are localised areas with a coating of droplet-like forms. No other surface deposits were observed……..25

Plate 27 Epifluorescence photographs showing the microbes observed in control samples CT2 (a) and 3 (b) 27

Plate 28 Epifluorescence photographs showing the microbes observed in biotic samples CTCO2-1 (a), CTCO2-9 (b) and CTCO2-11 (c).....28

TABLES

Table 1 Summary details of the sandstone core samples 5

Table 2 Whole-rock X-ray diffraction analysis of control samples 11

Table 3 Whole-rock X-ray diffraction analysis of biotic residues 12

Table 4 Mean total microbial counts by epifluorescence microscopy of outflow fluids from the control experiment. 26

Table 5 Mean total microbial counts by epifluorescence microscopy of outflow fluids from the biotic experiment 28

Table 6 pH measurements for control samples 30

Table 7 pH measurements for biotic samples 30

Summary

Work carried out by BGS and the Japan Atomic Energy Authority (JAEA) has shown that microbial processes can have profound effects on the transport properties of host rock (*i.e.* the movement of fluids and contaminants through the host material) relevant to radioactive waste disposal. Recent research, performed as part of the BGS Radtran project, has examined Sherwood Sandstone samples in the context of radioactive waste disposal; this particular formation is also a potential reservoir for carbon dioxide storage in the UK. As part of the BGS opportunities fund programme, this project has, for the first time, evaluated interactions between fluids saturated with carbon dioxide/Sherwood Sandstone/microbes (*Pseudomonas aeruginosa*) in transport experiments, using BGS developed apparatus under pressurised subsurface conditions. This pilot study has highlighted the impacts of differences in the physical characteristics of core Sherwood Sandstone samples collected adjacent to each other in a core sample, and the ability of *P. aeruginosa* to survive in CO_2 saturated artificial groundwater and the potential to form a biofilm in an environment suitable likely to be found at a carbon capture and storage location. These results demonstrate that in this short study, the injection of *P. aeruginosa* into the biotic experiment does not appear to impact on the physical transport properties of the Sherwood Sandstone, although the presence of CO_2 appears to enhance the mobilisation of a number of chemical species. However, in other work which utilised the same organism and rock type but without introduction of CO_2 saturated fluid, post-inoculation injection changes were observed. These included short but rapid saw-tooth like changes in the pressure profile (Wragg *et al*, 2012). These impacts were not observed in the current study which suggests that the CO_2 saturated fluid was impacting on the ability of the microbes to alter permeability. This short study has, however, indicated the need to carry out longer term investigations to reproduce these initial findings.

1 Introduction

The success of carbon capture and storage (CCS) projects depend on the ability of storage sites to contain CO_2 thus mitigating release to the atmosphere. However, concerns about the technology have been raised in many countries and have resulted in difficulties in implementing projects (*e.g.* onshore storage projects in the Netherlands). These concerns usually focus on the effects of possible leakages from storage sites and the potential large-scale environmental consequences of CCS. To date, studies have focused on the physical and chemical impact of CO_2 in stable geological formations, with associated monitoring systems to assure that no significant leakage occurs to the surface. If leakage was to occur after formal closure of the injection site, this could be over small areas from discrete point sources, such as abandoned wells, resulting in locally high concentrations of CO_2 in near-surface ecosystems. Consequently, environmental impacts of localised elevated CO_2 on terrestrial and marine ecosystems are areas of active research (*e.g.* West *et al,* 2006; Beaubien *et al,* 2008; Maul *et al,* 2009; Krüger *et al,* 2009; 2011). However a CO_2 storage site could also directly impact deep subsurface microbial ecosystems and biogeochemical processes.

It is well recognised that microbes can live in a wide range of subsurface environments where they have limited nutrient and energy supplies and exhibit very low metabolic rates (*e.g.* Lin *et al,* 2006; D'Hondt *et al,* 2002; West and Chilton, 1997). Thus it is almost certain that microbes will be found at depths considered for CO_2 storage and, consequently, that CO_2 storage sites may contain microbes that could be affected by injected CO_2 and any associated impurities such as NO_x, SO_x and H_2S. Whilst it is extremely unlikely that microbes could survive exposure to super-critical CO_2, many will survive and thrive in contact with the gas or dissolved phases (Morozova *et al,* 2010). The resulting impacts of microbial activity from these reactions could be both physical (*e.g.* altering porosity through the production of biofilms – Coombs *et al,* 2010) and chemical (*e.g.* changing pH, redox conditions) and may result in intracellular or extracellular mineral formation or degradation (Ehrlich, 1999; Milodowski *et al,* 1990; Mitchell *et al,* 2009; Tuck *et al,* 2006). These processes could all directly impact on the physical transport of CO_2 and/or impurities (as a gas or dissolved in fluid) through fractures and porous media. They could also have significant implications for groundwater quality, in terms of acidification and possible dissolution of minerals and mobilisation of elements (Kharaka *et al,* 2006), many of these reactions being known to be microbially catalysed (West *et al,* 2011).

The potential role of microbes in CO_2 storage was described by West *et al,* (2011) and has been identified by the Risk Assessment network of the International Energy Agency Greenhouse Gas Research and Development programme (IEA-GHG, June 2011) as an area that needs to be addressed (IEA-GHG report in preparation).

Work carried out by BGS and the Japan Atomic Energy Authority (JAEA), using BGS in-house developed apparatus, has shown that microbial processes can have profound effects on the transport properties of host rock (*i.e.* the movement of fluids and contaminants through the host material) relevant to radioactive waste disposal (Harrison *et al,* 2011). Recent research, performed as part of the BGS Radtran project, has examined Sherwood Sandstone samples in the context of radioactive waste disposal has also shown similar effects on the transport properties of this formation (Wragg *et al,* 2012). This particular formation is also a potential reservoir for CO_2 storage in the UK.

As a result of these findings, a pilot study was set up to evaluate, for the first time, the interactions between fluids saturated with CO_2, Sherwood Sandstone and the microbe (*Pseudomonas aeruginosa*) in transport experiments, using the BGS Biological Flow Apparatus

(BFA) under pressurised subsurface conditions. This report details the results from these experiments.

2 Laboratory techniques

2.1 EXPERIMENTAL OVERVIEW

The aim of this study was to evaluate how biofilms, generated by soil bacteria *P. aeruginosa*, influenced the flow of synthetic saline groundwater through intact Sherwood Sandstone. Two experiments, one biotic and the other an abiotic control, were carried out using BFA operated at a constant flow rate and under pressurised conditions. Changes in biological and chemical parameters were monitored throughout the experiment together with changes in confining pressure and temperature. The experiments were conducted over approximately 31 days and 89 days for the control and biotic experiments respectively, using sandstone samples taken from the Sherwood Sandstone Group from the Cleethorpes borehole (See Table 1). A saline groundwater (0.25M as NaCl) was prepared, supplemented with sodium acetate (0.25g l^{-1}) to provide a readily available source of organic carbon to promote and sustain microbial growth, as this pilot experiment was short-term (Table 1), and sterilised by filtration though a Sartorius filter (0.2 μm). For the biotic experiment the groundwater was saturated with carbon dioxide (CO_2). Outflow fluids were collected from both cores and analysed for their major and trace element chemistry, to investigate the microbial effects on migration.

For the control experiment (*i.e.* no injection of microorganisms), the apparatus was fully assembled and filled with artificial groundwater on 4th November 2011. The system was monitored until decommissioning on the 5th December 2011 giving a total run time of 31 days.

The biotic experiment was started on 8th December 2011 and was filled with artificial groundwater. The system was monitored until December 15th 2011, when the pump was re-filled with artificial groundwater saturated with CO_2, 7 days after the start of the experiment. This was followed by injection of *P. aeruginosa* on 18th January 2012, 41 days after assembly of the experiment. Pumping continued until the March 6th 2012. The pump was stopped and the experiment was decommissioned the next day – a total of 89 days from the beginning of the experiment.

2.2 FLOW-THROUGH COLUMN METHODOLOGY

The flow-through column experiments were performed using intact Sherwood Sandstone rock core. Core material was positioned vertically in a Teflon sheath with stainless steel end caps allowing fluid flow through the column and the assembly was then placed in a pressure vessel. Schematics of the completed experimental rig with the pressure vessel and rock core assembly are shown in Figures 1 and 2 with photographs of the assembled apparatus in Plates 1 and 2. Once assembled, the pressure vessel was partially filled with deionised water and pressurised to 4000 kPa (40 bar). The cores were not pre-saturated with synthetic groundwater prior to the start of the experiment. The synthetic saline groundwater was used to fill the syringe pump and the flow rate was set at 300 μl h^{-1} (~ 7.2 ml day^{-1}). The control column was not injected with the organisms and the test was run for 31 days. The synthetic saline groundwater in the 'biotic' column was replaced by CO_2 saturated synthetic saline groundwater 7 days after column assembly and the column injected with *P. aeruginosa* after a further 34 days. This experiment was terminated after a total of 89 days after assembly.

Pressure transducers, shown in Figure 1 as PT 1 and PT 2, were used to monitor the pressure changes within the cores while the syringe pumps controlled the flow-rate. The transducer outputs were recorded, along with actual pressure measurements on a calibrated DRUCK DPI 610 pressure calibrator and this data were subsequently used to calibrate the pumps and transducers. Fluid samples were collected by syringe at regular intervals for chemical and biological analyses.

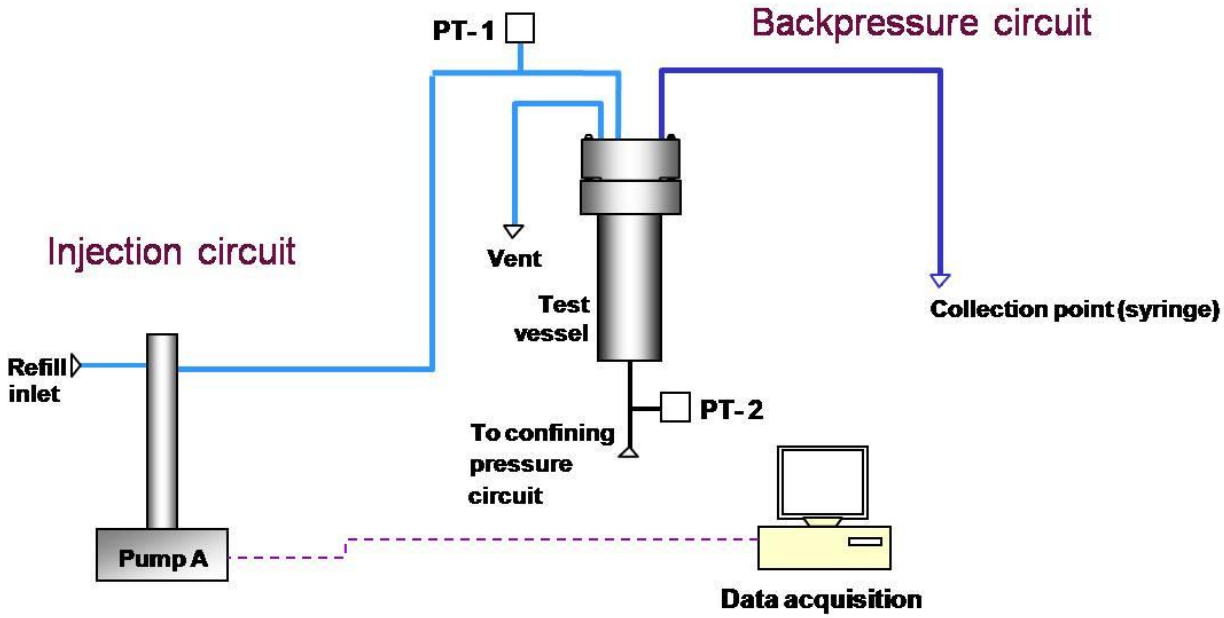

Figure 1 Schematic of column design

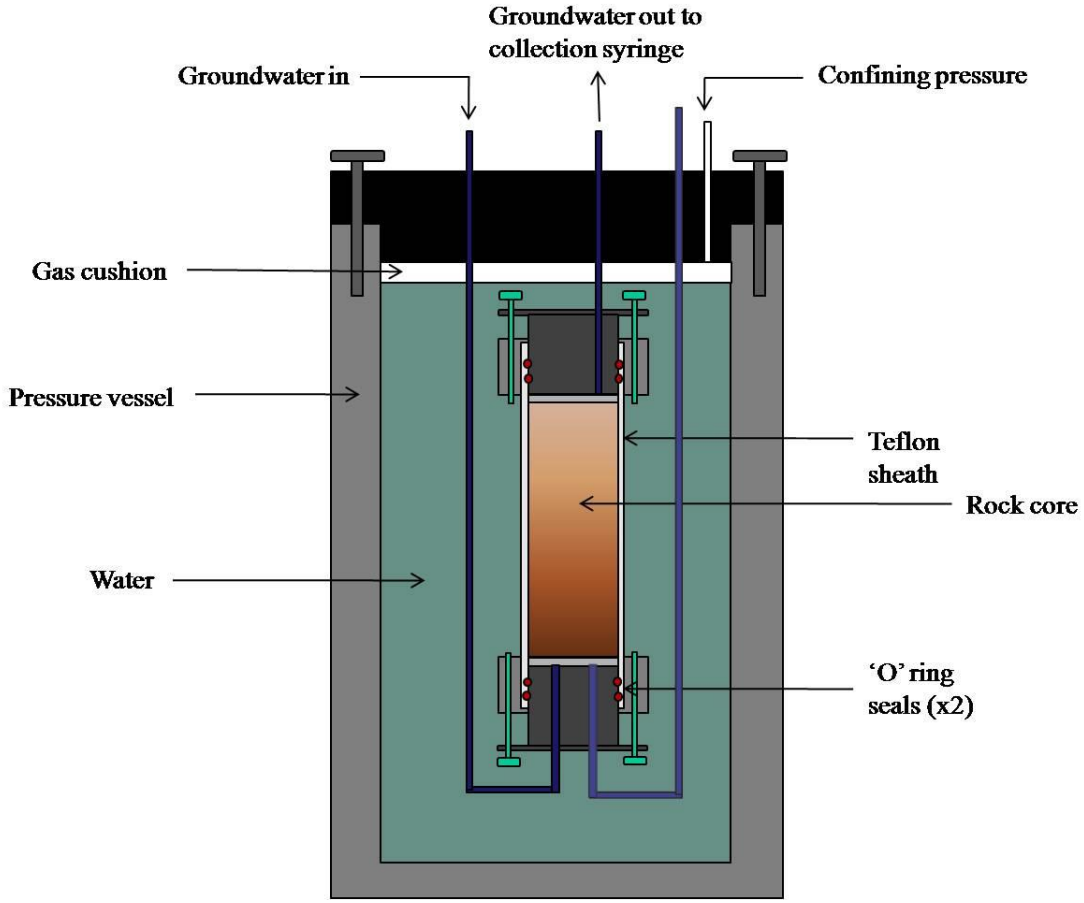

Figure 2 Schematic of pressure vessel with column containing rock core

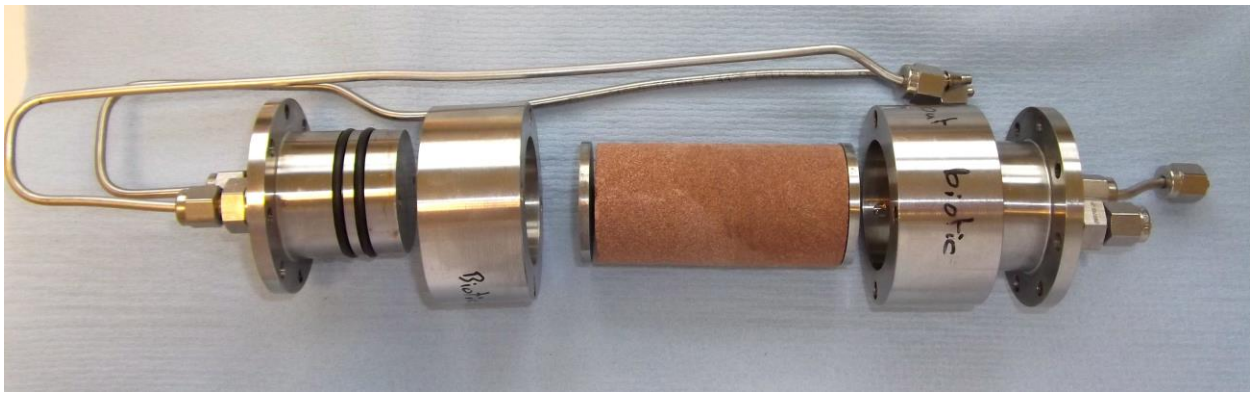

Plate 1 Photograph of column components prior to final assembly and insertion into pressure vessel

Plate 2 Photograph of assembled apparatus showing pressure vessel and syringe pump

2.3 PREPARATION OF FLUIDS

The synthetic groundwater was prepared from AR grade solid reagents. A saline (0.25M NaCl) solution was prepared by dissolving 14.6 g l^{-1} of NaCl in 18.4 ΩM water. Sodium acetate ($CH_3.COONa.3H_2O$) was added as 0.25 g l^{-1} (TOC = 22 mg l^{-1}). The fluid was then filter sterilised using a 0.2 µm filter and refrigerated until assembly of the experiment. Synthetic groundwater saturated with CO_2 was prepared by bubbling CO_2 at 1 atmosphere through the fluid for 24 h prior to injection on to the column.

2.4 SELECTION AND PREPARATION OF INTACT CORE MATERIAL

Based on background BGS information on the Sherwood Sandstone Group (Milodowski and Rushton, 2008) and previous studies as part of the BioTran project, investigating biofilm formation on samples from the Sherwood Sandstone Group (West *et al*, 2011), a sandstones with appropriate permeability characteristics from the Cleethorpes No.1 borehole was identified for use in this study. To produce the samples, parallel plugs were longitudinally cut from the MPLP510 sample core using a 37 mm (nominal) diameter (ID) diamond-impregnated core barrel. The sample details are provided in Table 1.

Table 1 Summary details of the sandstone core samples

Borehole	Stratigraphy	Rock Type	Sample Depth (m)	Sample Code	Experiment
Cleethorpes No. 1 Lincolnshire	Sherwood Sandstone Group (undifferentiated)	Feldspathic sandstone	1312.26-1312.41	MPLP510	Control and Biotic

2.5 BACTERIAL CULTURE

P. aeruginosa was selected for its biofilm (exopolysaccharide - EPS) forming properties (Vaughan *et al*, 2001) and has been used previously in BioTran experiments (Harrison *et al*, 2009). It is a gram-negative rod, 0.5 to 0.8 µm wide by 1.5 to 3.0 µm in length and is a pathogen to humans. The matrix of the *P. aeruginosa* biofilm is composed of an alginate polymer of mannuronic and glucuronic acids. Its natural habitat is soil but it is also common to water and vegetation. *P. aeruginosa* is primarily aerobic but will grow under anaerobic conditions in the presence of nitrate which it can use as a respiratory electron acceptor; it is also resistant to high concentrations of salts. In this respect, it is a suitable strain for the experiment as synthetic saline groundwater is being utilised.

P. aeruginosa (NCIMB 10548) was received in a freeze dried state and resuscitated by adding 0.5 ml of sterile Nutrient broth (OXOID). This suspension was then sub-cultured onto agar slopes (OXOID CM3) and into a 50 ml flask of sterile nutrient broth. The slopes were refrigerated to maintain a stock culture for future experiments. The flask was placed on an orbital shaker, and incubated overnight at 36ºC, to encourage microbial growth. After 24 h the actively growing culture was then further inoculated into 500 ml flasks of sterile nutrient broth to achieve a large volume of bacteria. The culture was then transferred to 35 ml sterile tubes and centrifuged at 4600 rpm for 20 minutes. The supernatant was aseptically removed and the volume replaced with sterile artificial saline groundwater. The tubes were remixed and the centrifugation process repeated four times until all traces of culture media were 'washed' from the bacteria. Decreasing volumes of synthetic groundwater were added at each stage to concentrate the bacteria. The resulting fluid was then added to approximately 500 ml of synthetic groundwater, this produced sufficient volume to fill the syringe pump. A 1 ml sample of each suspended culture was removed by sterile pipette and preserved in gluteraldehyde fixative solution (Jass and Lappin-Scott, 1992) prior to microscopic examination. The total number of bacteria inoculated was then determined by direct counting using epifluorescence microscopy (Hobbie *et al*, 1977; Jass and Lappin-Scott, 1992).

2.6 DECOMISSIONING OF EXPERIMENTS

The control experiment was terminated on 5th December 2011 with decommissioning of the biotic experiment on 6th March 2012. Plate 3 shows the decommissioning procedure. Plates 4 and 5 show the intact control and biotic columns prior to opening for mineralogical analyses, the direction of flow is indicated by arrows.

Plate 3 Example of column assembly removal from pressure vessel

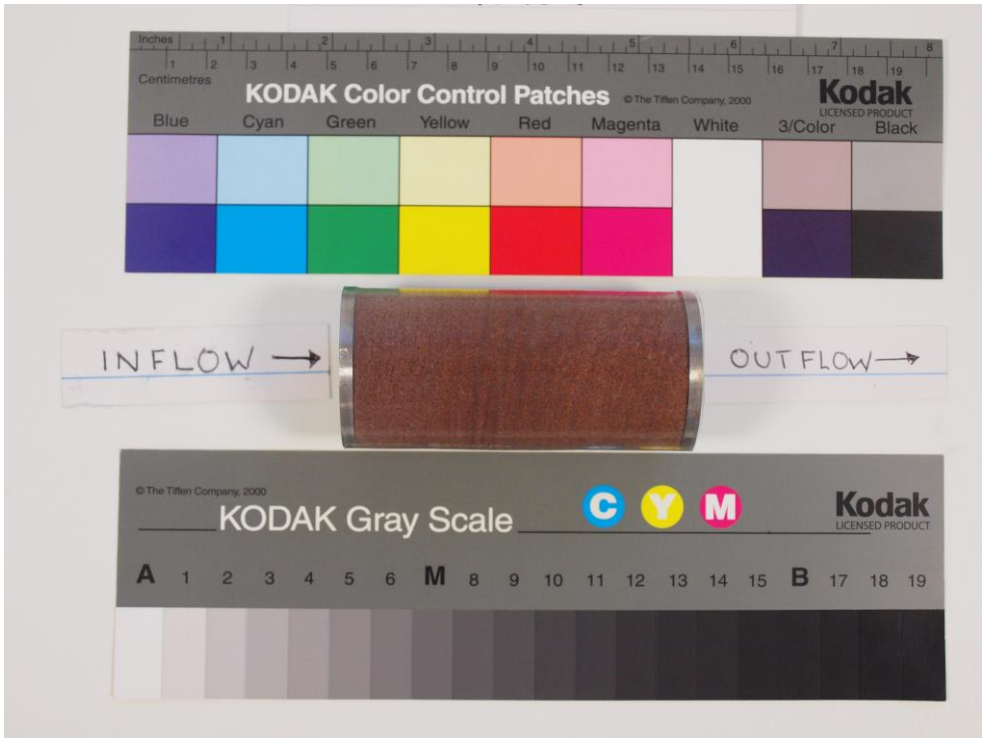

Plate 4 Control column after removal from pressure vessel and end pieces. Arrows indicate direction of fluid flow during the experiment

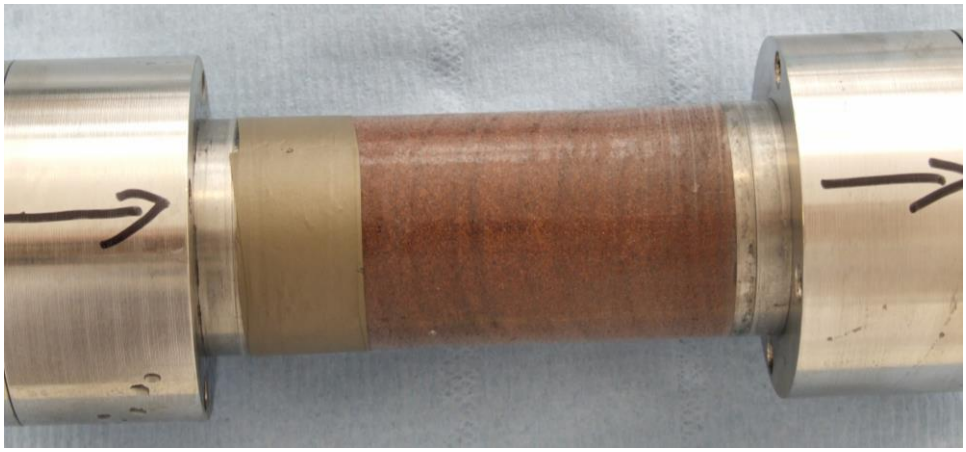

Plate 5 Biotic column after removal from pressure vessel. Arrows indicate direction of fluid flow during the experiment

3 Analytical techniques

3.1 CHARACTERISATION OF SOLID MATERIALS

3.1.1 X-ray diffraction analyses

Quantitative whole-rock mineralogical analysis and qualitative clay mineral analysis of the post-experimental control materials and biotic residues were determined by X-ray diffraction (XRD) analysis.

3.1.1.1 SAMPLE PREPARATION

The samples were initially ground in a pestle and mortar. In order to achieve a finer and uniform particle-size for whole-rock XRD analysis, a 2.7 g portion of each ground material was micronised under acetone for 10 minutes with 10 % (0.3 g) corundum (American Elements - PN:AL-OY-03-P). The addition of an internal standard allows to validate quantification results and also to detect any amorphous species present in the samples. Corundum was selected as its principle XRD peaks are suitably remote from those produced by most of the phases present in the samples. The samples were then back-loaded into standard stainless steel sample holders for analysis.

Approximately 5 g of each crushed sample was dispersed in deionised water using a reciprocal shaker combined with ultrasound treatment. The suspensions were then sieved on 63 µm and the <63 µm materials placed in a measuring cylinder and allowed to stand. In order to prevent flocculation of the clay crystals, 1 ml of 0.1M 'Calgon®' (sodium hexametaphosphate, Sigma-Aldrich (305553)) was added to each suspension. After a time period determined from Stokes' Law, a nominal <2 µm fraction was removed and dried at 55°C. Only small quantities of <2 µm materials were removed from the samples. The <2 µm materials were re-suspended in a minimum of distilled water and Ca-saturated by adding a few drops of 1M $CaCl_2.6H_2O$ solution. The Ca-saturated suspensions were then pipetted onto the surface of a 'zero-background' silicon crystal.

3.1.1.2 QUANTITATIVE X-RAY DIFFRACTION ANALYSIS

XRD analysis was carried out using a PANalytical X'Pert Pro series diffractometer equipped with a cobalt-target tube, X'Celerator detector and operated at 45kV and 40mA.

The micronised samples were scanned from 4.5-85°2θ at 2.76°2θ min^{-1}. Diffraction data were initially analysed using PANalytical X'Pert Highscore Plus version 2.2a software coupled to the latest version of the International Centre for Diffraction Data (ICDD) database.

Following identification of the mineral species present in the samples, mineral quantification was achieved using the Rietveld refinement technique (*e.g.* Snyder & Bish, 1989) using PANalytical Highscore Plus software. This method avoids the need to produce synthetic mixtures and involves the least squares fitting of measured to calculated XRD profiles using a crystal structure databank. Errors for the quoted mineral concentrations are typically ± 2.5% for concentrations >60 wt%, ± 5% for concentrations between 60 and 30 wt%, ±10% for concentrations between 30 and 10 wt%, ± 20% for concentrations between 10 and 3 wt% and ± 40% for concentrations <3 wt% (Hillier *et al*, 2001). Where a phase was detected but its concentration was indicated to be below 0.5%, it is assigned a value of <0.5%, since the error associated with quantification at such low levels becomes too large.

The <2 µm oriented mounts were scanned from 2-40°2θ at 1°2θ min^{-1} after air-drying, after glycol-solvation and after heating to 550°C for 2 hours.

3.1.2 Petrography

3.1.2.1 Sampling and Sample Preparation

The post-experiment control and biotic samples were removed from the flow test apparatus contained within their polytetrafluoroethylene (PTFE) sleeves and with end frits in place. In each case, the contained plugs were then immersed in sterile 0.25M NaCl brine (sterilised by filtration at 0.25 µm), that also contained 0.25 g l^{-1} of sodium acetate. The PTFE sleeves and end frits were subsequently removed and the plugs re-immersed in the sterile brine. Any prolonged storage was under refrigerated conditions (<6˚C).

Sub-sampling for the various solid material analyses was performed by briefly removing the samples from the brine. The biotic sample was split longitudinally with half being retained for petrographic analyses and half taken for microbiology testing and characterisation.

For scanning electron microscope (SEM) analysis, samples were taken as rock chips from carefully noted positions along the length of the cores. For the Biotic core, the chips were taken from central and edge sites at each position.

3.1.2.2 Scanning electron microscopy procedures

The assessment of the solid experimental materials was carried out using an FEI Company Quanta 600 environmental scanning electron microscope (ESEM) equipped with an Oxford Instruments INCA Energy 450 energy-dispersive X-ray microanalysis (EDXA) system with a 50 mm2 peltier-cooled (liquid nitrogen free) silicon drift detector (SSD) X-ray detector capable of detecting elements from boron to uranium. The EDXA system is used as a guide to mineral phase identification.

The ESEM was used in environmental mode: the pressure of the SEM chamber in this operating mode is held at pressures in the region of 500-750 Pa (4-6 Torr). At these pressures using an H_2O atmosphere and with a cooled stage it is possible to keep water in the liquid state at the sample surface. This is illustrated in Figure 3, the phase diagram for water. Adjustment of temperature and pressure with reference to this water phase diagram then allows control of the theoretical sample humidity, with 100% representing the 'dew point' and values <100% resulting in evaporation and drying of water in a controlled manner.

To give good control over the chamber and sample conditions, the sample needs to be small so that there is minimal thermal lag, and thermal conductivity between the sample materials and the cooled stage needs to be good. To fulfil these requirements with rock samples, the sample must

be small (mm scale) and should be mounted in a saturated state within a small reservoir of liquid. The sample holder used for this is a small aluminium cup (Plate 6 a & b). In this study, distilled water was used as the added liquid reservoir.

Typical ESEM operating procedures were as follows. The sample was mounted in the peltier cooled stage Initial pumping of the sample chamber was performed with no purge, with target conditions set to 100% humidity at ~2˚C. Initial beam conditions were 7.5-10.0 kV accelerating voltage at spot size 5. Typical optimal working distance was 5-7 mm.

During ESEM analysis, all samples were exposed to a range of carefully controlled temperature and pressure changes to observe the way in which pore-lining fluids changed during drying episodes. Drying episodes were also used to reveal the nature (composition, morphology) of residues in an attempt to identify their origins (mineral, biotic, solution precipitate).

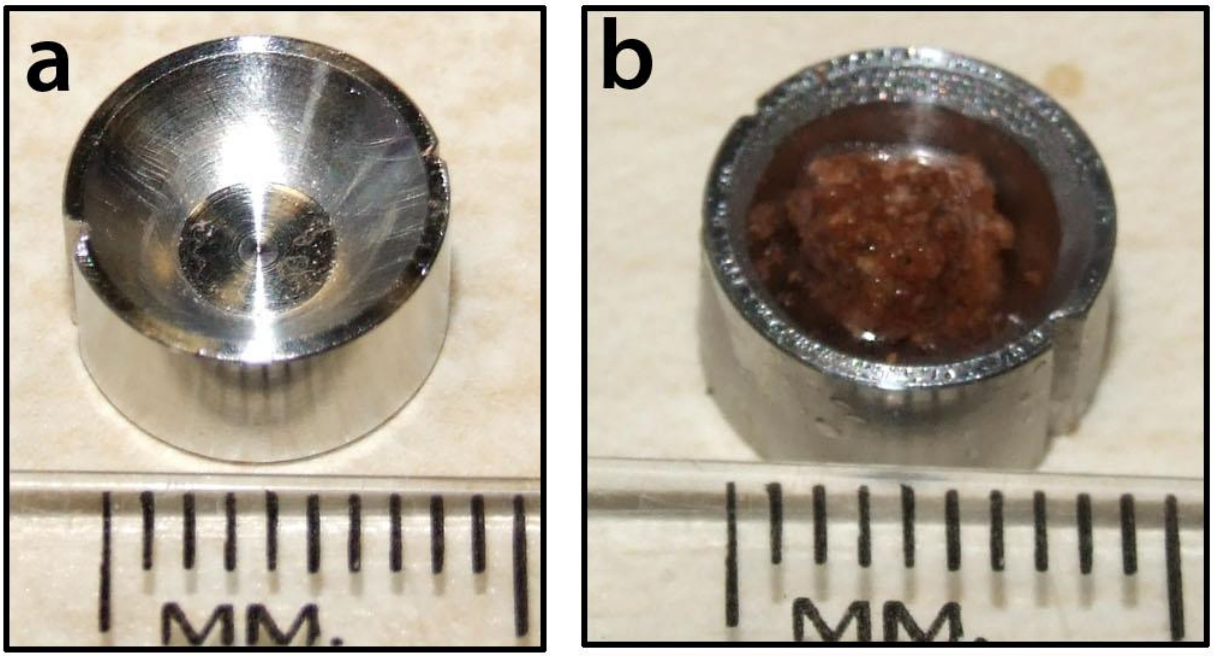

Plate 6 ESEM sample holders and preparation. a: cup holder used for rock chips. b: example cup with mm scale rock chip and pool of liquid.

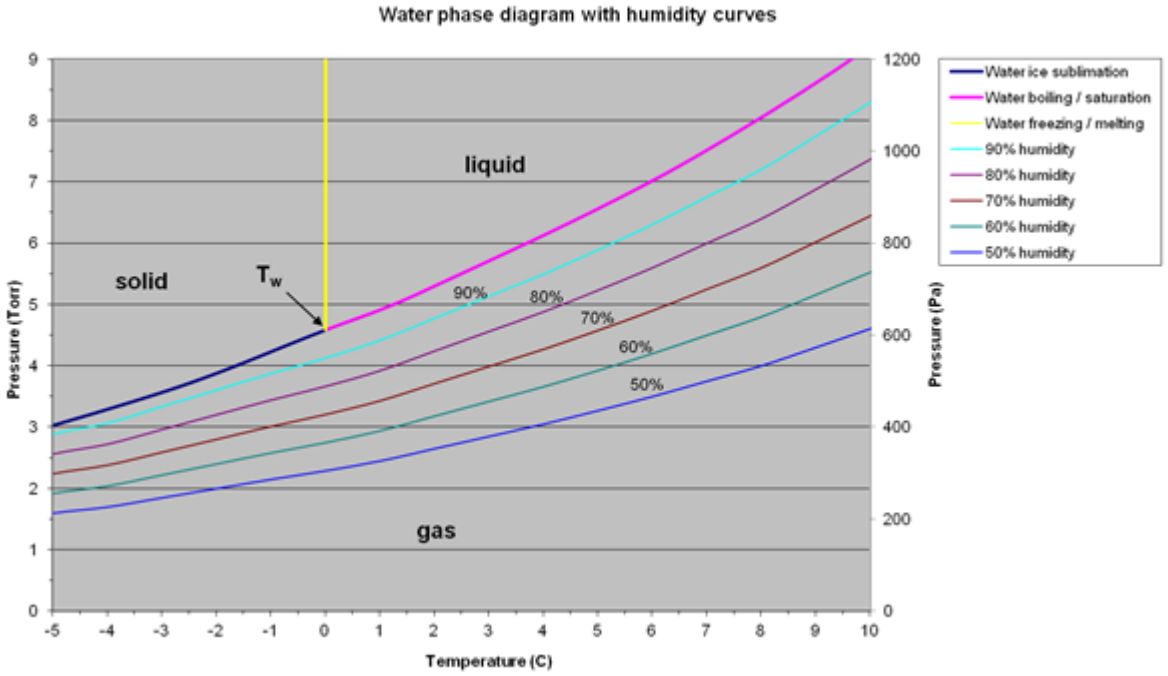

Figure 3 P/T phase diagram for water in the region relevant to ESEM operation. Tw is the triple point. Source data for the sublimation and melting curves has been derived from Wagner *et al.* (1994), and for the boiling / saturation curve is *IAPWS formulation for industrial use, 1997*. Humidity curves have been calculated and superimposed on the gas portion of the diagram.

3.2 MICROBIAL ANALYSES

A reference sample of the synthetic groundwater used to fill the syringe pump was taken for comparison to the outflow fluids from the biotic and control columns at the start of each test (day 0) and at approximately 7 day intervals until the end of the experiments. Microbial biomass was evaluated using epifluorescence microscopy. Epifluorescence microscopy uses a short wavelength transmission source to fluoresce a sample stained with the nucleic acid selective cationic fluorochrome. The fluorescent stain, Acridine Orange, or N,N,N',N'-tetramethylacridine 3,6-diamine ($C_{17}H_{19}N_3$), was used to determine total cell counts (Hobbie *et al*, 1977; Jass and Lappin-Scott, 1992). Acridine Orange is capable of permeating cells and interacting with DNA and RNA by intercalation or electrostatic attractions. When the fluorescent stain interacts with DNA, which is spectrally similar to fluorescein, the excitation maximum is at 502 nm (cyan) and the emission maximum at 525 nm (green), while RNA interactions shift the excitation maximum to 460 nm (blue) and the emission maximum to 650 nm (red). Thus, it is possible to determine if cells are metabolically active as they appear red due to the predominant RNA whereas inactive or slow growing microbes have mostly DNA and appear green. By examination of 20 randomly selected fields of view, the numbers of organisms per ml can be counted.

3.3 CHEMICAL ANALYSES

A reference sample of the artificial groundwater used to fill the syringe pump was taken for comparison to the outflow fluids from the biotic and control columns at the start of each test (day 0) and at 7 day intervals until the end of the experiments. Chemical analyses included major anions by ion chromatography, (IC) and cations by Inductively Coupled Plasma - Optical Emission Spectroscopy, (ICP-OES), as well as redox sensitive species (Fe^{2+}/Fe^{3+}), pH and selected microbial nutrients (e.g. C, P, S and N). Non-Purgeable Organic Carbon (NPOC) was

also determined, which gives an indication of the degradation rate of organic compounds during the experiments.

4 Results

4.1 CHARACTERISTICS OF THE SANDSTONE STARTING MATERIALS

4.1.1 X-ray diffraction analysis

The starting material has previously been analysed and the results reported by West *et al*., (2011). In summary, the sample comprises of major amounts of quartz, minor amounts of feldspars (K-feldspar and plagioclase) and 'mica' (undifferentiated mica species possibly including muscovite, biotite, illite, illite/smectite etc) and trace amounts of chlorite and hematite. The clay fraction (<2 μm) is composed of illite, illite-smectite mixed-layer clay and chlorite.

4.2 CHARACTERISTICS OF THE POST-EXPERIMENTAL MATERIALS

4.2.1 Whole rock mineralogical analysis results

The results of whole-rock XRD analyses of the post-experimental control samples and biotic residues that were taken at 10-20 mm intervals along the column are summarised in Tables 2 and 3.

XRD analysis showed that the samples are predominantly composed of quartz, minor amounts of feldspars (K-feldspar and plagioclase), dolomite and 'mica' (undifferentiated mica species possibly including muscovite, biotite, illite, illite/smectite *etc*.) and trace amounts of chlorite, halite and hematite. Trace amounts of amphibole were detected in the biotic residue at 0-10 mm from column inlet.

No significant differences between the control materials and biotic residues were detected.

Table 2 Whole-rock X-ray diffraction analysis of control samples

Subsamples taken from column inlet in mm	MPL Code	Mineralogy (%)							
		albite	chlorite	dolomite	halite	hematite	K-feldspar	'mica'	quartz
0 - 20	MPLQ632	4.8	0.6	4.7	<0.5	<0.5	12.8	1.8	74.7
20 - 40	MPLQ633	5.4	0.6	5.3	<0.5	<0.5	12.3	2.4	73.4
40 - 60	MPLQ634	5.0	<0.5	5.5	<0.5	<0.5	12.9	1.9	73.9
> 60	MPLQ635	4.4	<0.5	5.8	<0.5	<0.5	13.0	1.8	74.3

Table 3 Whole-rock X-ray diffraction analysis of biotic residues

Subsamples taken from column inlet in mm	MPL Code	Mineralogy (%)								
		albite	amphibole	chlorite	dolomite	halite	hematite	K-feldspar	'mica'	quartz
0 - 10	MPLQ861	4.6	<0.5	0.8	5.5	<0.5	<0.5	13.3	2.0	73.2
10 - 20	MPLQ862	4.8	nd	0.7	5.2	<0.5	<0.5	13.6	1.8	73.5
30 - 40	MPLQ863	4.8	nd	0.7	4.5	<0.5	<0.5	13.5	2.0	74.2
40 - 60	MPLQ864	5.0	nd	0.5	4.5	<0.5	<0.5	13.1	2.0	74.6
> 60	MPLQ865	5.2	nd	0.5	5.5	<0.5	<0.5	12.7	2	73.7

Key

nd – not detected

'mica' = undifferentiated mica species including muscovite, biotite, illite and illite/smectite etc.

4.2.2 Clay Mineralogy

The results of XRD analysis of the <2 μm materials of the control samples and biotic residues showed that the clay mineral fraction is composed of illite, illite-smectite mixed-layer clay and chlorite.

The biotic sample residues at '0-10 mm' and 10-20 mm' from column inlet also exhibited a small peak at *c.* 16.7Å after ethylene glycol salvation, suggesting the presence of trace amounts of smectite (estimated <1% of the clay fraction). This was observed neither in the original core samples nor in any of the control samples and may be linked to the introduction of microbes. However, longer duration experiments are needed to make definitive conclusions, as it is possible that this is just an artefact of sample heterogeneity (*e.g.* laminations within the sandstone).

A labelled clay mineral XRD trace of the biotic sample taken at '0-10 mm' is shown in the Appendix.

4.2.2.1 NON-SWELLING CLAYS

The 'non-swelling clays' illite, and chlorite were identified in all the samples:

Illite was identified by its characteristic air-dry *d*001 spacing of *c.*10.0Å which remains invariant after glycol-solvation and heating.

Chlorite was identified by its characteristic air-dry and glycol-solvated basal spacing peaks at 14.2, 7.1, 4.73 and 3.54Å and particularly the presence of a peak at *c.*13.5Å after heating at 550°C.

4.2.2.2 SWELLING CLAYS

The illite/smectite detected in the samples is characterised by a broad *d*001/002 peak at *c.*11.6Å on the air dry trace and a peak at *c.*12.8Å on glycol-solvation. Heating to 550°C causes the peak to collapse to a *c.*9.6Å spacing.

4.3 PETROGRAPHY

4.3.1 Control Sample

Samples were analysed from the inlet end of the post-test control plug and from 40-50 mm into the sample from the inlet face. Plates 7 to 12 are example SEM images of the post control test material.

At the inlet end, some pore walls were observed to be thinly and patchily coated by a film-like phase. This film was typically associated with deposits of silicate fines. These fines were either mobilised during testing or by post-testing sample preparation. In detail the film locally has a fibre-like content. Under the electron beam of the SEM and at ESEM chamber humidities <100%, the film was noted to shrink, suggesting it has a high water content. Rare cell-like textures were noted as <2 µm rounded forms on pore walls.

A similar film was also identified at the 40-50 mm depth within the post-test sample material, although of considerably reduced abundance. Again, the film locally has a filamentous content, is associated with silicate fines, and shrinks under the electron beam and at reduced humidities. No cell-like features were identified, however.

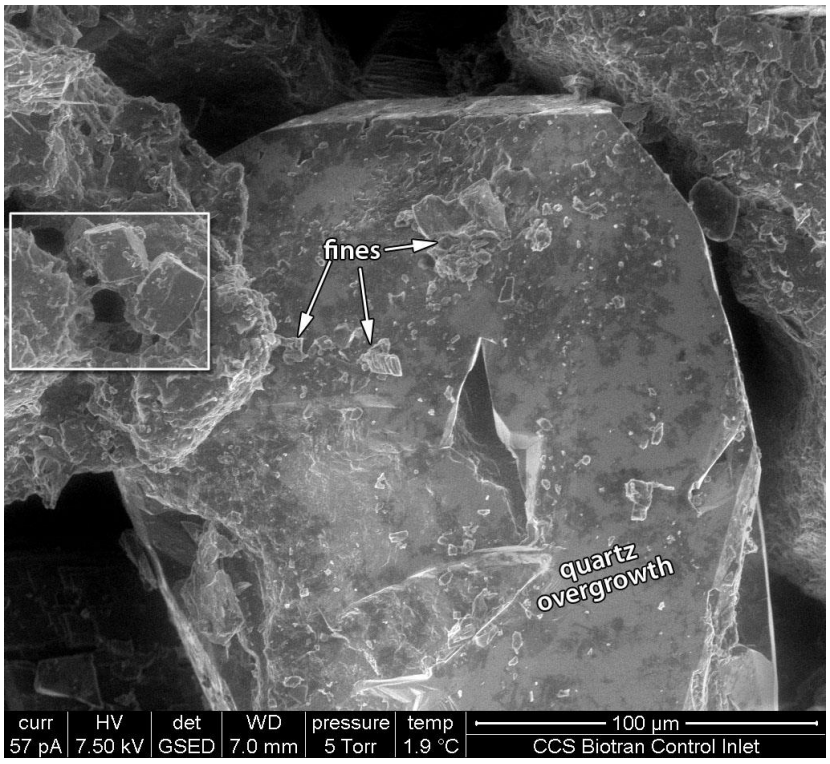

Plate 7 SEM image. Post test control sample, inlet end, 95% humidity. A patchy dark film-like deposit on the pore walls, much of it here defined by quartz overgrowth, is typically associated with deposits of mobilised fines. Boxed area is the site of the following plate.

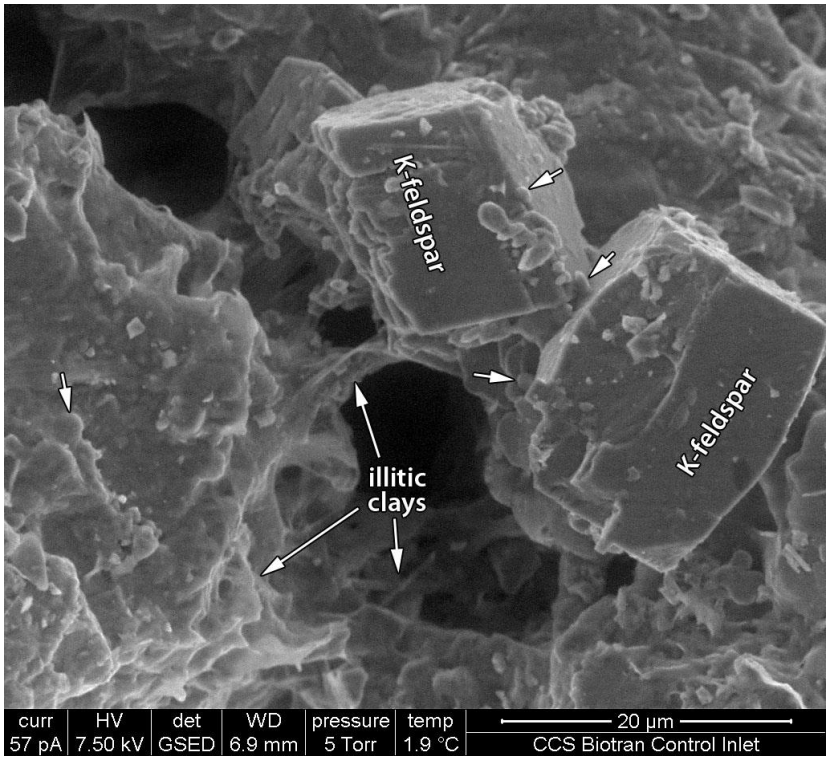

Plate 8 SEM image. Post test control sample, inlet end, 95% humidity. From the boxed area in the preceding image. Diagenetic features include authigenic K-feldspars and illitic clays bridging a pore throat. There are scattered oval and rounded forms about 2 µm across scattered on pore walls.

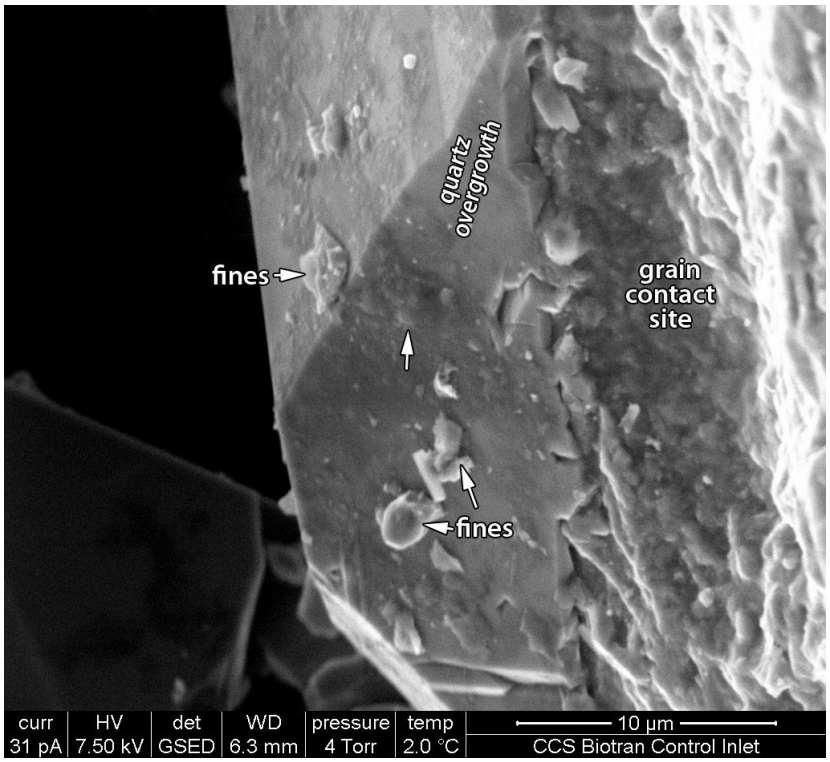

Plate 9 SEM image. Post test control sample, inlet end, 80% humidity. A quartz overgrowth is partially coated by a thin film-like phase. There are mineral fines deposited on the surface of the film.

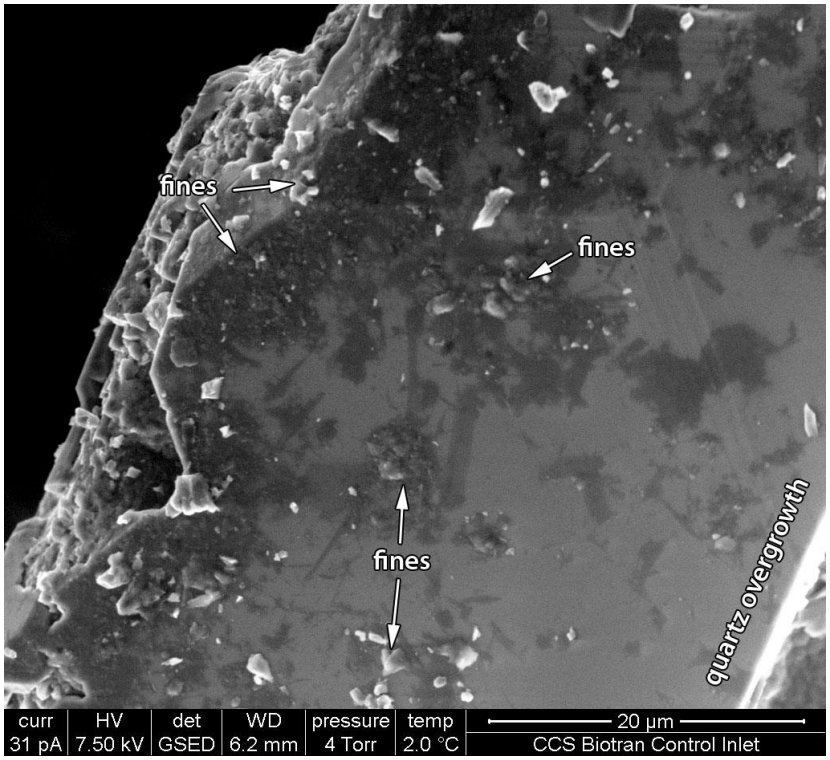

Plate 10 SEM image. Post test control sample, inlet end, 80% humidity. A quartz overgrowth is partially coated by a thin film-like phase, commonly with a filamentous form. There are widespread mineral fines deposited on the surface of the film.

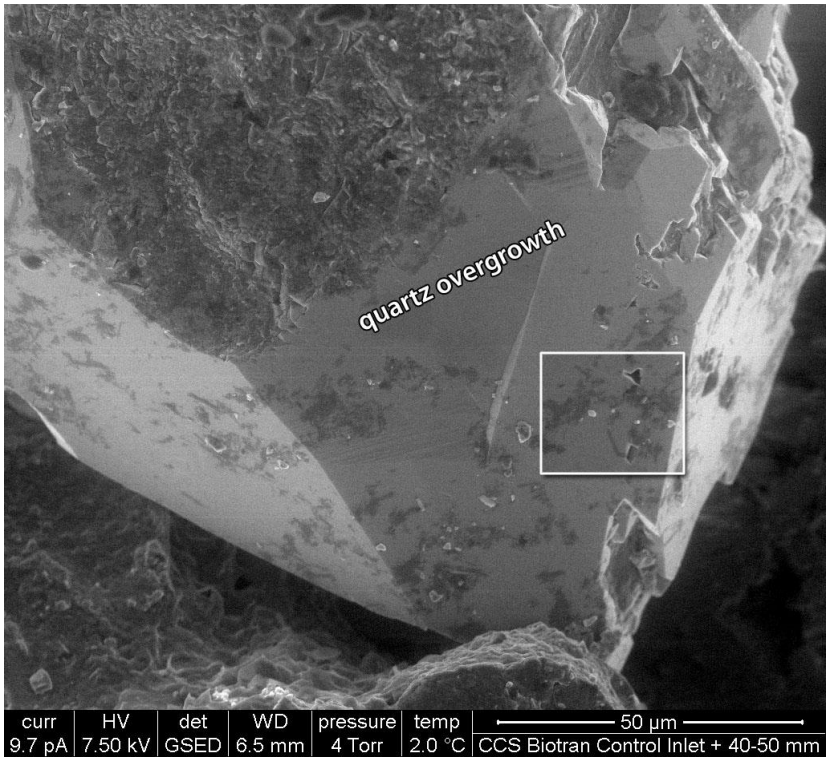

Plate 11 SEM image. Post test control sample, from 40-50 mm beyond the inlet face, 80% humidity. Pore walls, here defined by quartz overgrowth, have a sparse and patchy film-like coating. Boxed area is the site of the following plate.

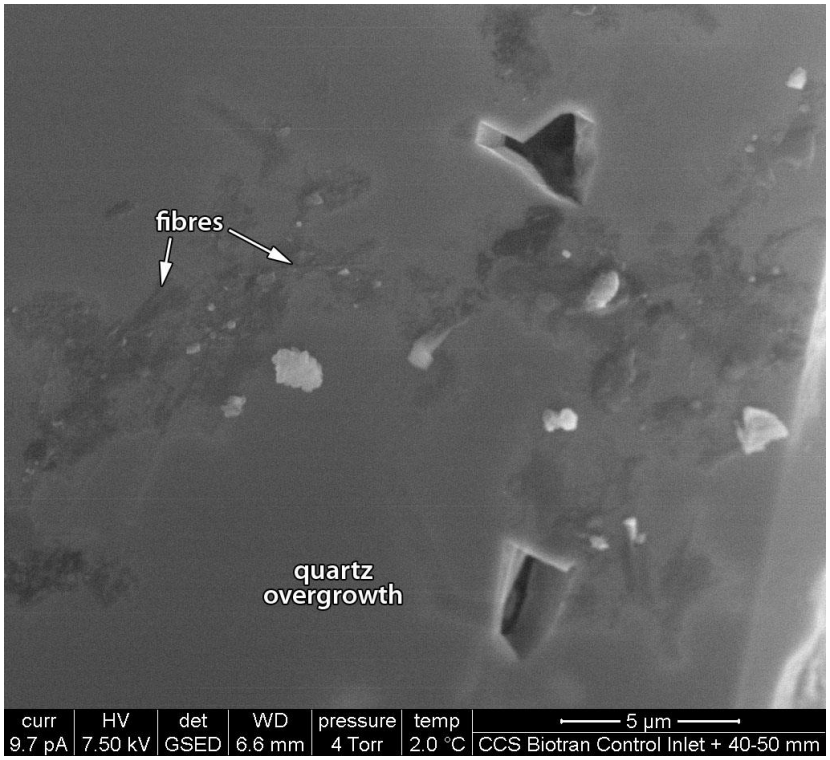

Plate 12 SEM image. Post test control sample, from 40-50 mm beyond the inlet face, 80% humidity. Detail of the patchy film-like coating from the boxed area in the preceding plate. Again, the film is typically associated with fines. In detail the film commonly has a fibrous aspect.

4.3.2 Biotic Sample

Upon removal of the biotic sample from the test apparatus, it was noted that a portion of the test plug had a grey stain visible at its outlet end (Plate 13, Plate 14 and Plate 15). Upon splitting the plug as part of the sample preparation, it was further noted that this staining was only present at the outside surface; it did not appear to have penetrated the sample to any significant depth (Plate 16).

Samples were taken and analysed from the inlet end of the post-test biotic plug, from 40 mm into the sample from the inlet face, and from the outlet end. At each of these sampling points, samples were prepared from the centre and from the edge of the plug. One edge sample from the outlet end was prepared to include an area affected by the grey staining to enable this to be examined.

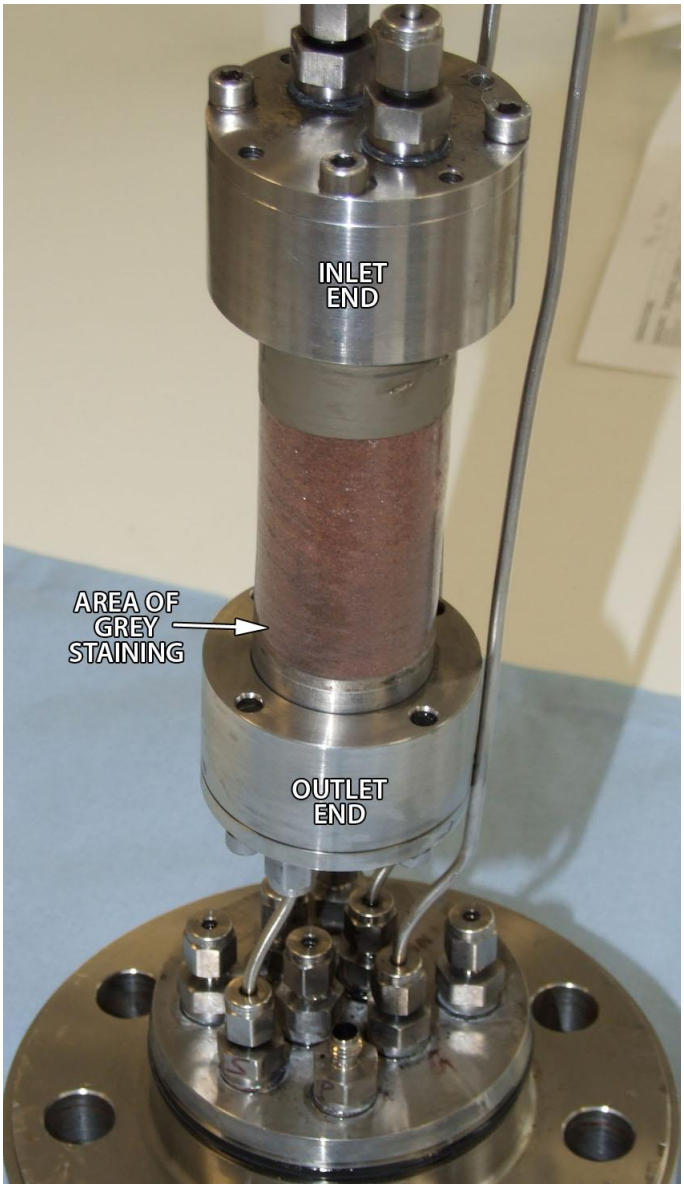

Plate 13 Biotic sample during decommissioning, showing the test plug contained in the apparatus. An area of grey staining is apparent at the outlet end of the plug.

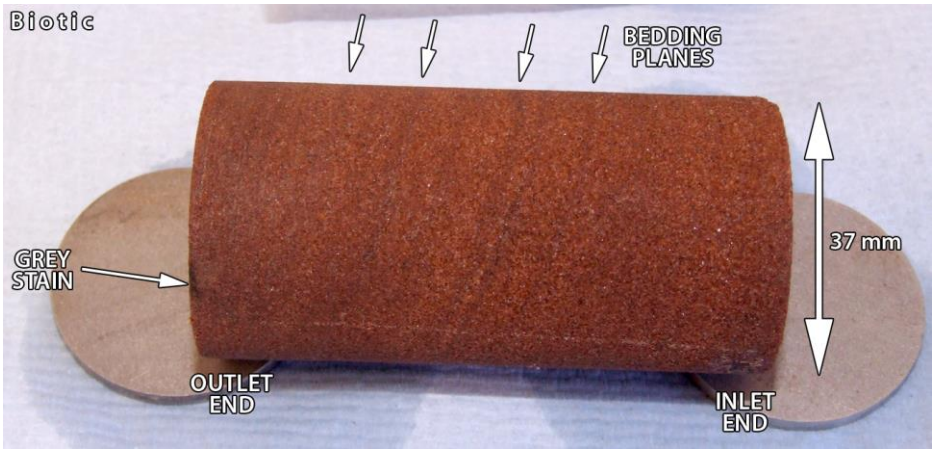

Plate 14 Test plug and end frits after removal of the outer casing, showing the patch of grey stain on the outside at the outlet end. Bedding planes are indicated.

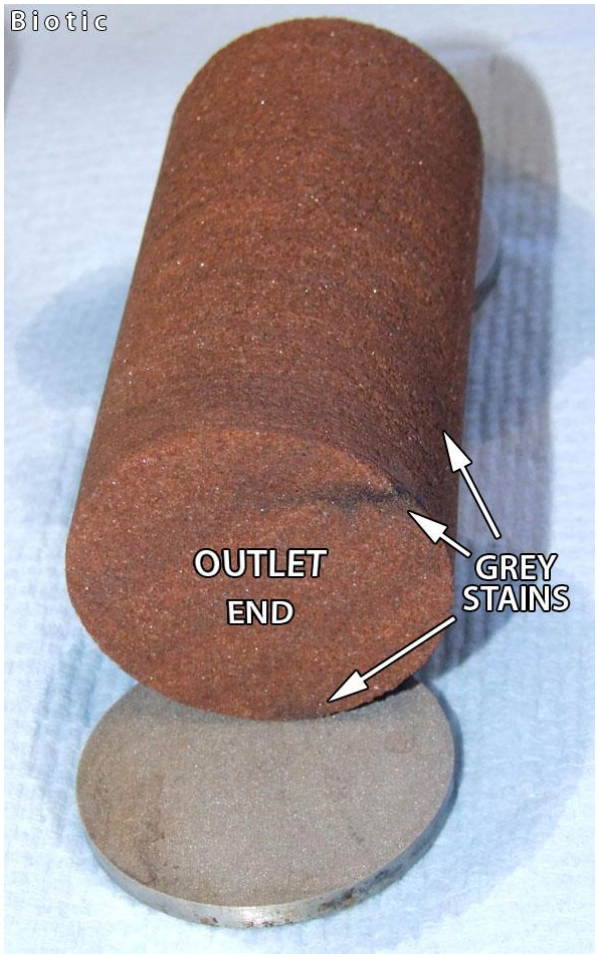

Plate 15 Outlet end of the test plug showing the extent of the grey staining.

Plate 16 Biotic test plug freshly fractured, showing the strongly defined bedding structures. The grey staining observed on the outside of the plug has not penetrated the plug interior.

4.3.2.1 INLET END

At the inlet end most pore walls were observed to be thinly and patchily coated by a film-like phase (Plate 17 to Plate 20). This film was typically associated with collections of silicate fines that appear to be affixed by the film (Plate 19). These fines were either mobilised during testing or by post-testing sample preparation. Under the electron beam and at ESEM chamber humidity's <100%, the film was noted to shrink, suggesting it has a high water content. There are widespread cell-like textures associated with many of the patches of film, typically embedded as <3 µm oval, rounded forms (Plate 19, Plate 20).

In detail the film locally has a fibre-like content (Plate 18). These fibres are similar to a diagenetic fibrous illite locally recognisable as a grain-coating (Plate 25) and pore-bridging constituent of the host rock.

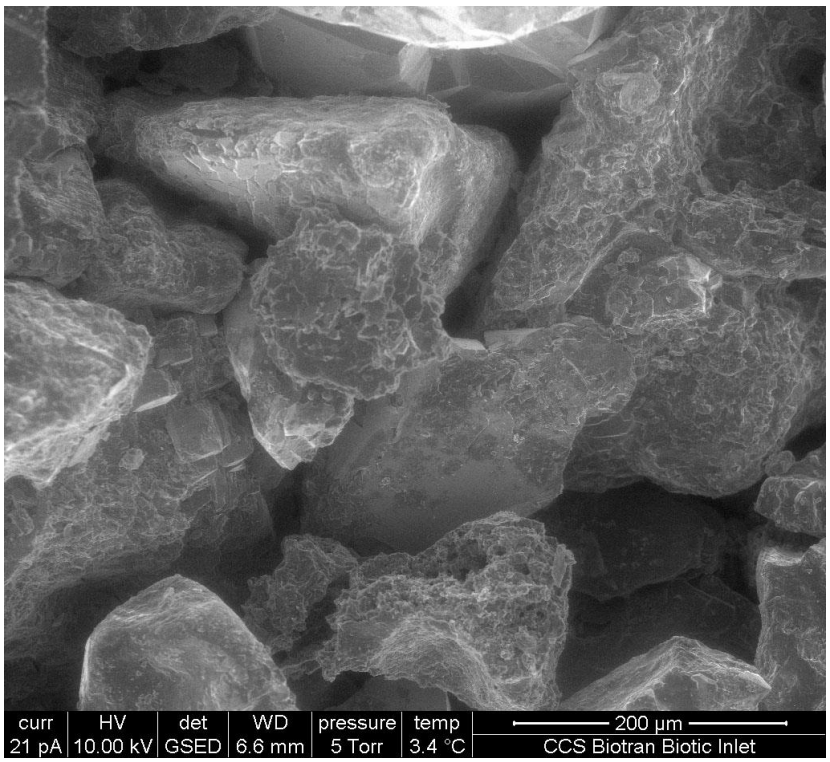

Plate 17 SEM image. Post test biotic sample, central inlet end, 90% humidity. General view showing scattered patches of a film-like deposit on pore walls, several with associated silicate fines.

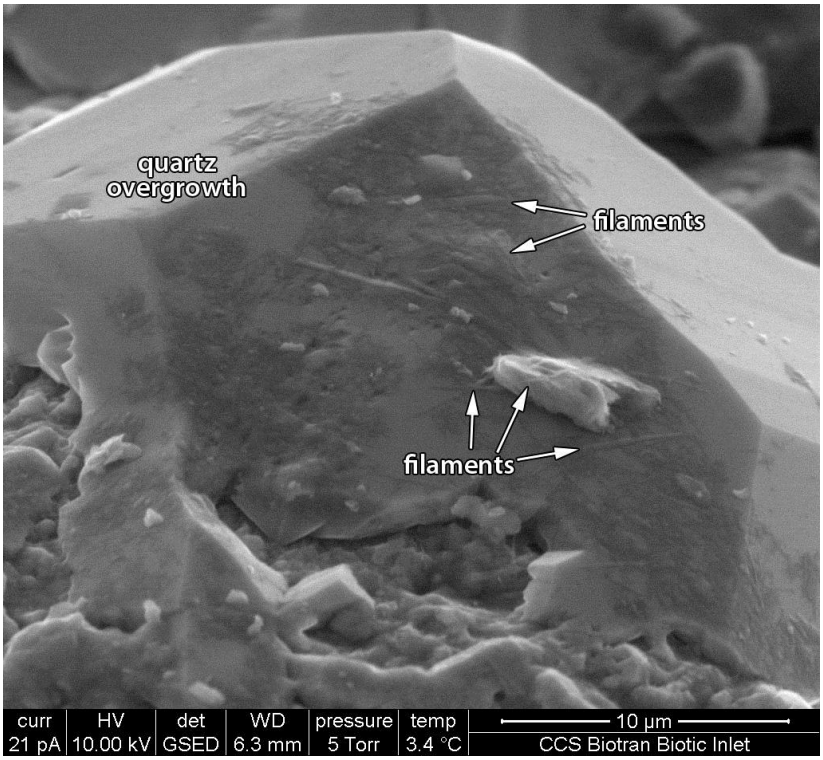

Plate 18 SEM image. Post test biotic sample, central inlet end, 90% humidity. Detail of a quartz overgrowth with a patchy film-like deposit. A filamentous phase associated with the film is also visible draped over the top of an angular fragment of silicate. This is most likely a fibre of illitic clay.

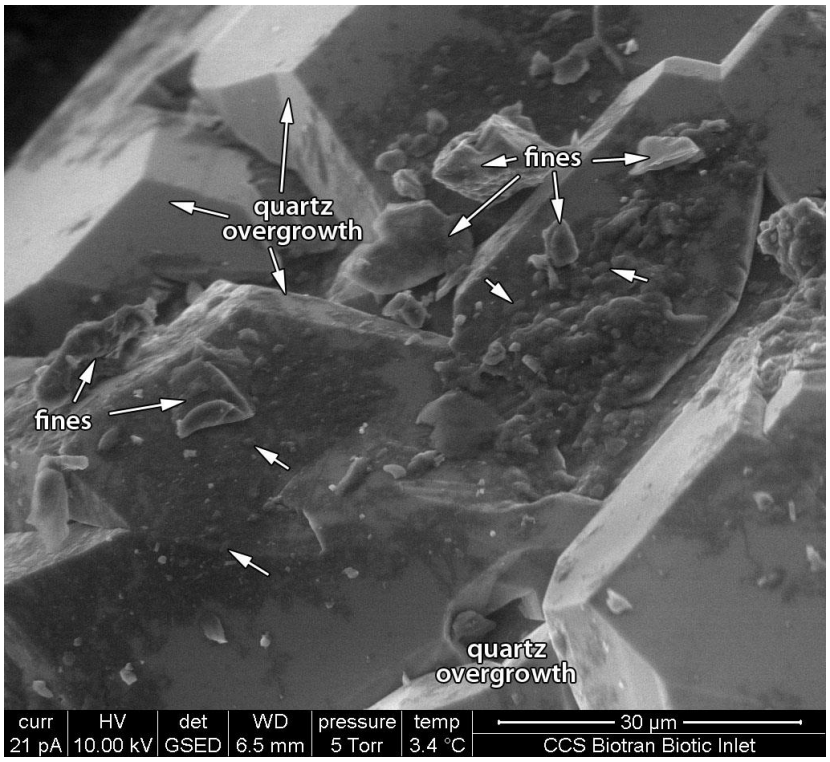

Plate 19 SEM image. Post test biotic sample, central inlet end, 90% humidity. This area of pore wall defined by quartz overgrowth is partially coated by film and associated fines. There are scattered rounded oval forms <3 µm across visible within the film (unlabelled arrows).

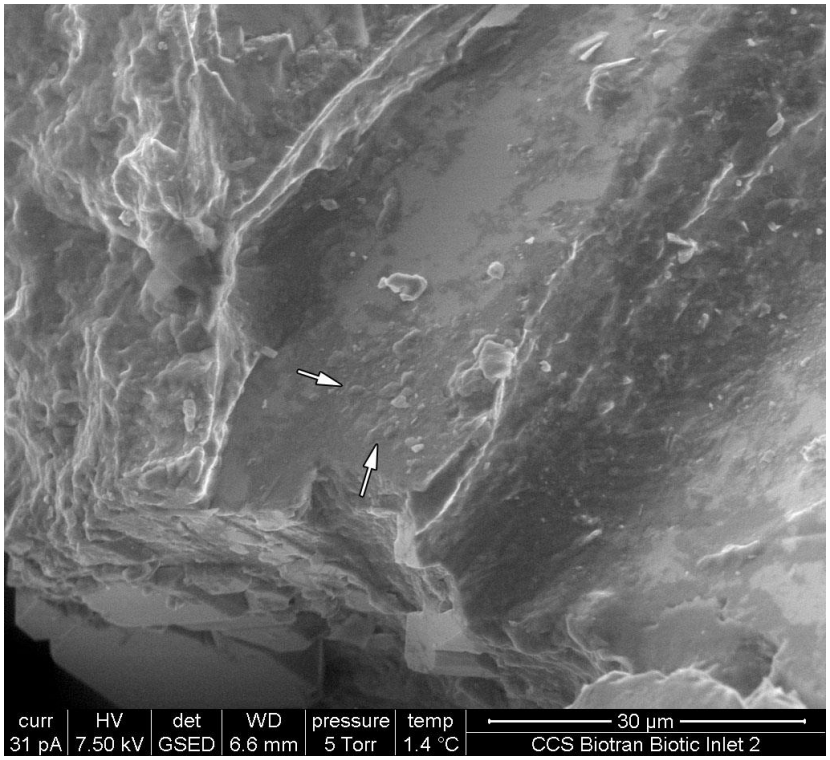

Plate 20 SEM image. Post test biotic sample, edge inlet end, 90% humidity. This area of pore wall has a patchy film coating that contains common rounded, oval <3 µm forms (unlabelled arrows).

4.3.2.2 INLET + 40 MM

A similar film to that observed in the inlet material was identified at the 40 mm depth point within the post-test sample material (Plate 21), with a slightly reduced abundance. Again, the film is typically associated with apparently adhered silicate fines (Plate 21 and 22), and shrinks under the electron beam and at reduced humidities. Cell-like features were rarely identified (Plate 22). Film was identified both in the central and edge samples.

At some sites where pore walls extend towards the centres of pores, film and associated fines appear to be more abundant (Plate 22); these sites are likely to have been extending into more rapidly moving test fluids.

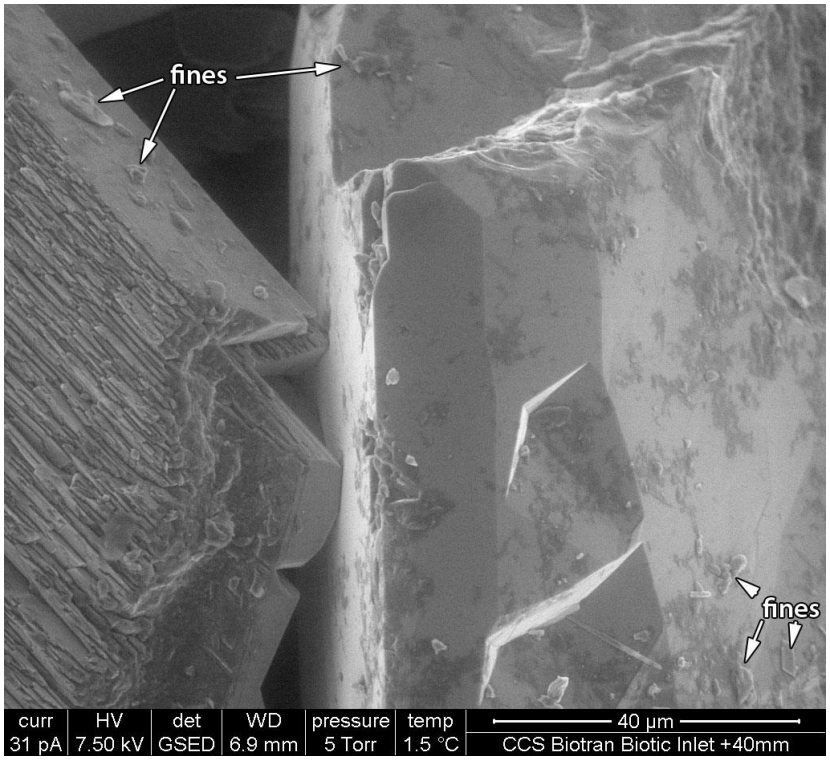

Plate 21 SEM image. Post test biotic sample, central inlet + 40 mm, 95% humidity. Typical patchy pore lining film with associated fines on quartz (centre, right) and K-feldspar (left) overgrowth faces.

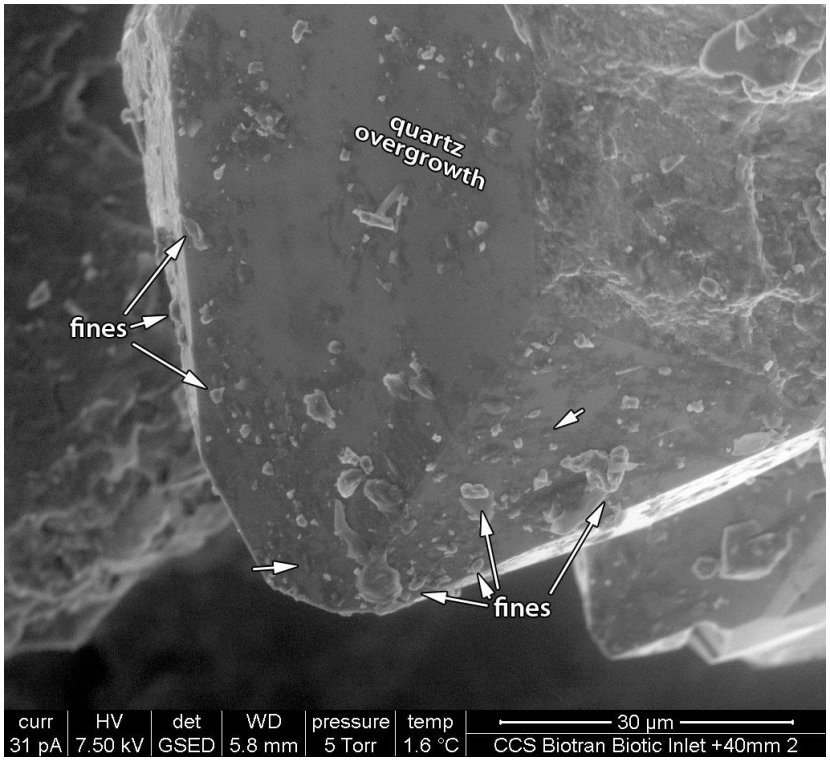

Plate 22 Post test biotic sample, edge inlet + 40 mm, 95% humidity. Patchy film and associated fines on a protruding apical quartz overgrowth site. Film and fines are more abundant towards the tip. There are scattered rounded, oval <3 µm forms (unlabelled arrows).

4.3.2.3 OUTLET

Film-like material similar to that observed in the rest of the sample is sparse, but identifiable at the outlet end both in central and edge (Plate 23) sites. No cell-like forms were recognised, however.

Examples of collapsed illitic fibres identified in the absence of film (Plate 24) show that the collapse is not necessarily related to the presence or formation of the film. Additionally, the presence of clusters of un-collapsed illitic fibres (Plate 25) shows that not all of this phase was collapsed state prior to testing, and that testing and analysis have not necessarily caused collapse.

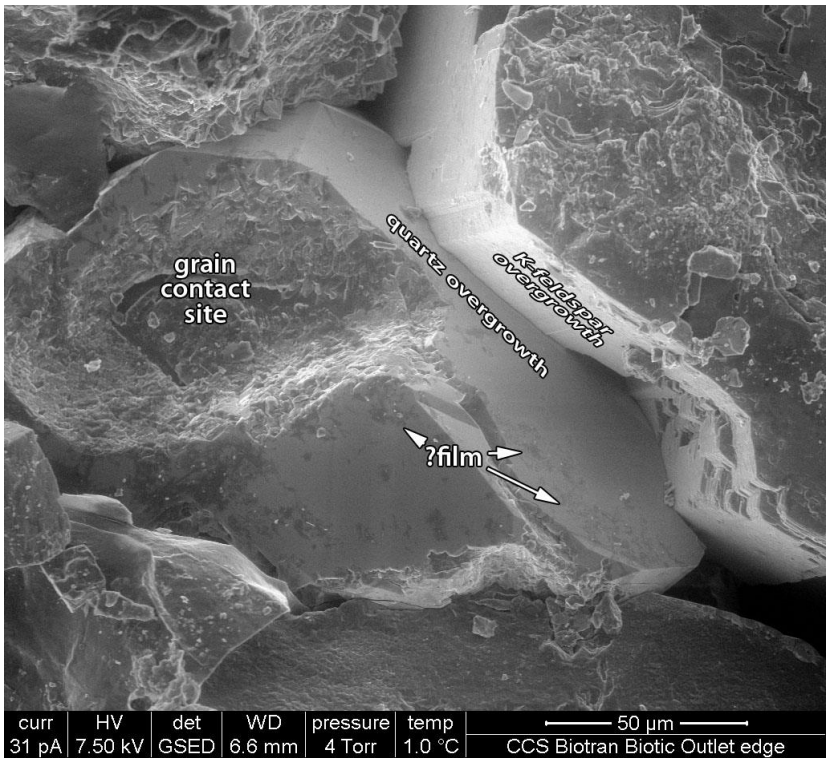

Plate 23 Post test biotic sample, edge outlet, 90% humidity. Pore-lining film is sparsely distributed at the outlet end of the sample both the edge sites (as shown here) and at central sites.

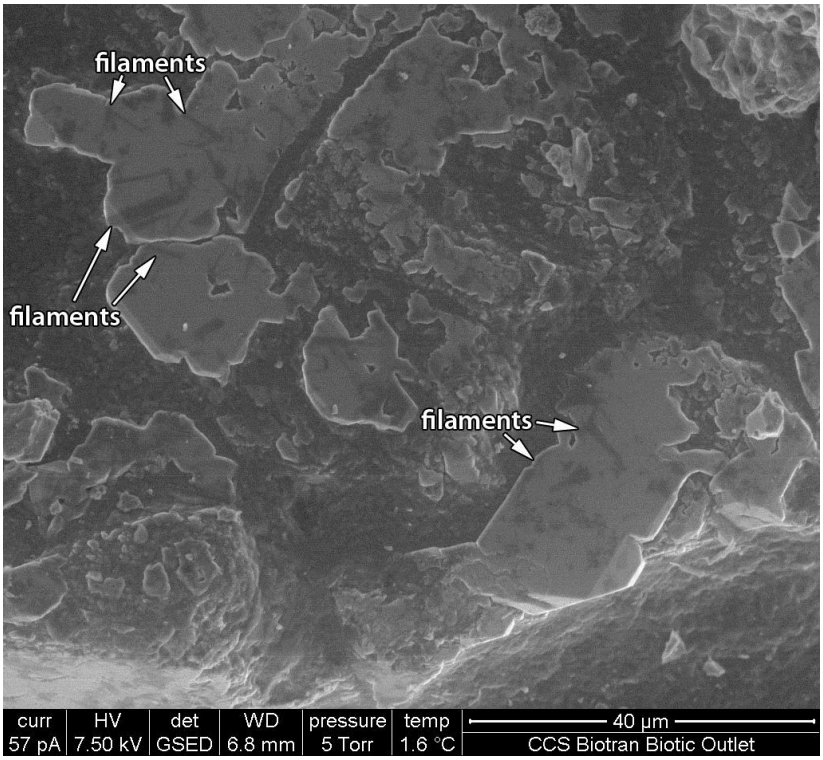

Plate 24 Post test biotic sample, central outlet, 90% humidity. Dark areas here are residual fluids on rougher pore walls and filamentous forms laid across a partially developed quartz overgrowth. These are illitic clay forms that are laid across the overgrowth surfaces; this probable collapse could have occurred prior to, during or after the testing.

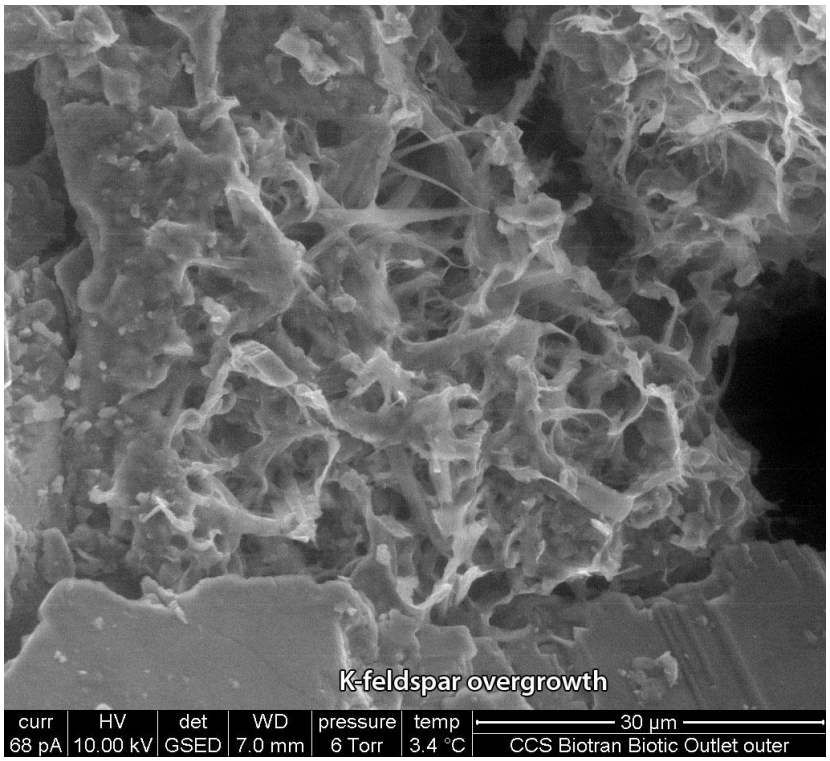

Plate 25 Post test biotic sample, edge outlet, 95% humidity. An example of a filamentous illitic clay cluster that has not collapsed. There is no evidence of film amongst the filaments.

4.3.2.4 GREY STAINED MATERIAL

A sample prepared from the area of the outlet end of the post test plug with the grey stain was examined. Small patches of a surface coating with a droplet like morphology were noted (Plate

26). Droplets ranged from 10-20 µm in diameter. These droplets appear to be of a non-aqueous liquid phase, since they did not evaporate under reduced humidity conditions.

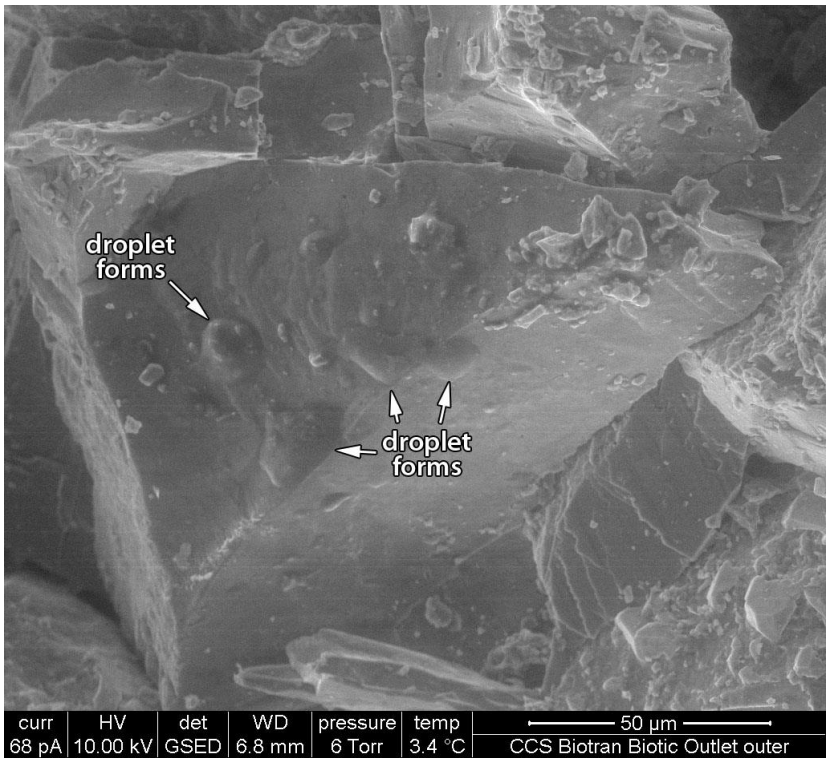

Plate 26 SEM image. Post test biotic sample, outlet end, grey stained area, 95% humidity. A sample portion prepared from the outer grey stained surface. There are localised areas with a coating of droplet-like forms. No other surface deposits were observed.

4.4 MICROBIOLOGY

Mean total microbial counts, obtained by epifluorescence microscopy, for the fluids from the control (abiotic) and biotic experiment experiments are given in Tables 2 and 3 respectively.

4.4.1 Control column experiment

The control column experiment ran for 31 days (744 h) in total with no injection of live organisms, pressure changes were continuously monitored throughout the course of the test. Table 4 and Figure 4 show the microbial count observed in the control experiment and indicate that although no live organisms were added to the experiment, indigenous microbes were present. The mean microbial count over the duration of the experiment peaked at 426 h, however the number of microbes observed was not considered to be significantly different to those observed on previous or latter sampling days. The visual difference in microbial counts is shown in Plate 27. The residual fluid in the pump at the end of the experiment indicated a high microbial count. This is thought to be a result of contamination of the experimental procedure or indigenous microbes from the test core breeding in the nutrient rich fluid. Microbial migration from the core to the pump requires further investigation.

Table 4 Mean total microbial counts by epifluorescence microscopy of outflow fluids from the control experiment.

Sample Name	Sampling Date	Total Time (h)	Mean organisms ml^{-1}	Standard Error
Start up fluid	03/11/2011	0.00	0	0
CT1	08/11/2011	89.33	2.09×10^6	2.00×10^5
CT2	15/11/2011	257.33	2.40×10^6	1.12×10^6
CT3	22/11/2011	425.83	9.22×10^5	1.28×10^5
CT4	29/11/2011	594.49	2.64×10^4	2.83×10^4
*Fluid in pump	06/12/2011	761.33	2.41×10^6	1.00×10^6

* Denotes microbial counts for fluid in the pump at the close of the experiment.

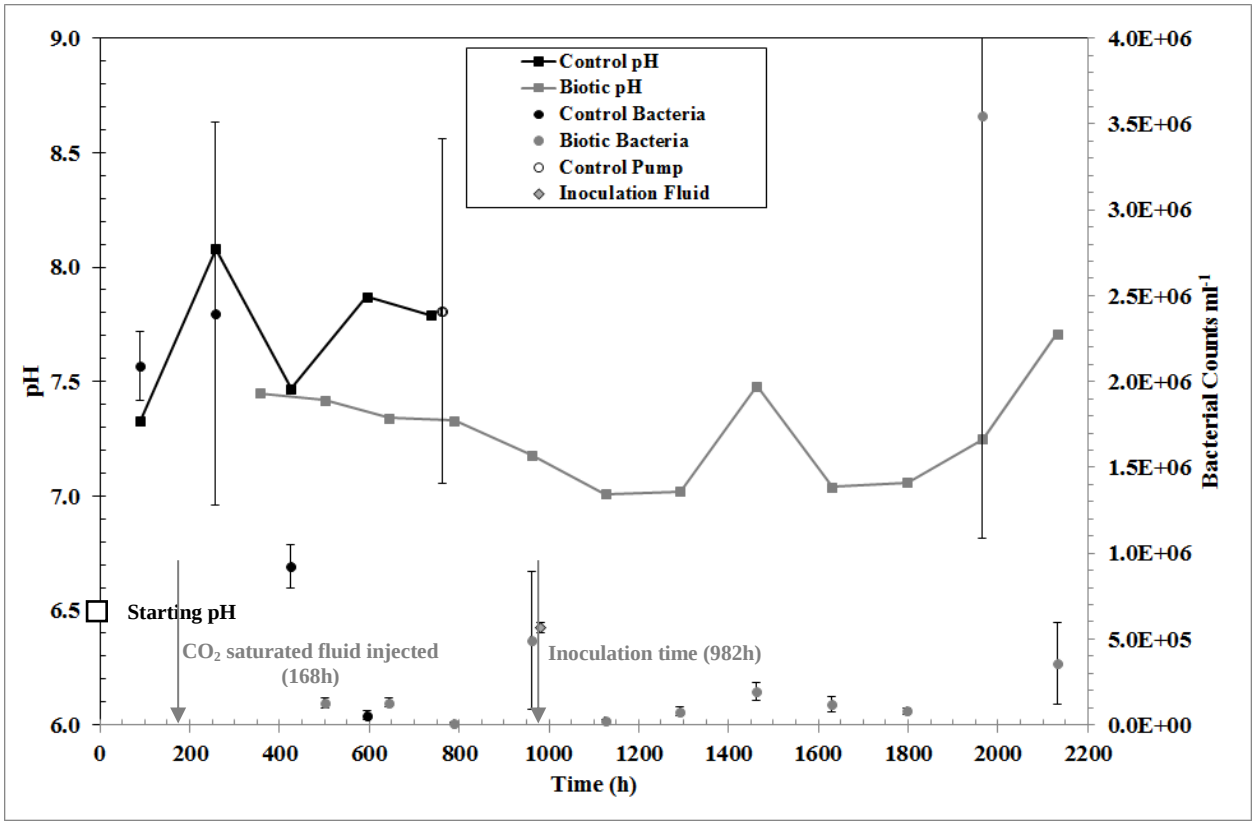

Figure 4 Microbial count and pH data for the control and biotic experiments. The control pH and microbial counts are shown by a black line a closed circles respectively with the biotic experiment represented by grey closed circles and line. The pH of the starting fluid in both experiments is shown by an open grey square. The number of microbes in the pump at the end of the control experiment are shown by an open black circle. The number of microbes in the inoculant for the biotic experiment are denoted by a closed grey diamond.

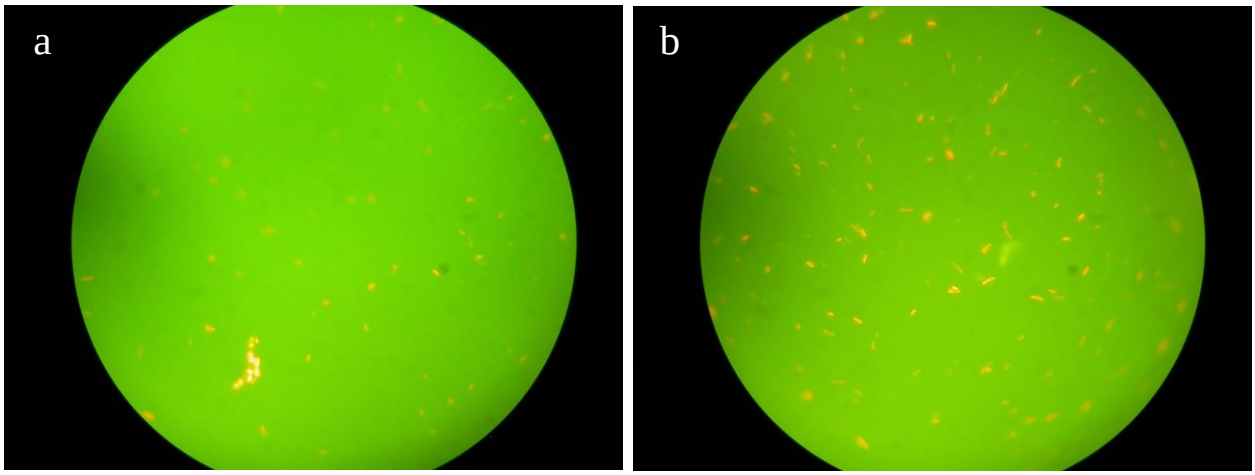

Plate 27 Epifluorescence photographs showing the microbes observed in control samples CT2 (a) and 3 (b)

4.4.2 Biotic column experiment

Sterile artificial groundwater was pumped through the core assembly for a nominal period (7 days – approx. 168 h) before the pump was stopped and CO_2 saturated groundwater injected. After a further 34days, and a total of 41 days (981 h) after the start of the experiment, the pump was stopped again and the *P. aeruginosa* bacteria injected.

Table 5 summarises the mean microbial counts collected from the outflow of the BFA at regular time intervals and the microbial count of the inoculant. Plate 28 shows epifluorescence images of samples CTCO-1, 9 and 11. Both Table 5 and Plate 28 indicate that the *P. aeruginosa* can survive in saline fluid saturated with CO_2. Examination of Plate 28 also shows differences in microbes with time. Plate 28(a) shows a relatively even spread of microbes at *circa*. 500 h, which has altered to a centralised mass of microbes, with other fluorescing material, that no longer covers the whole microscopic view at 1630 h (Plate 28 b). At 1965 h into the biotic experiment, a loose mass of microbes were observed, central to the microscopic view, with few surrounding mircrobes (Plate 28 c). Rod-like microbes were also observed, which were tentatively identified as bacillus.

Comparison of the number of viable microbes in the biotic experiment compared to the control experiment (Figure 4) indicates that the presence of CO_2 may restrict microbial activity. Subjective observation of the data presented in Plates 27 (b) and 28 (a) indicates that more microbes may be present in the biotic experiment thereby contradicting the microbial count data reported in Tables 4 and 5, which reports higher counts in the control experiments. This may be a function of the organisms clumping and therefore being more difficult to evaluate.

Table 5 Mean total microbial counts by epifluorescence microscopy of outflow fluids from the biotic experiment

Sample Name	Sampling Date	Total Time (h)	Mean organisms ml^{-1}	Standard Error
CTCO2-1	23/12/2011	354.94	1.16×10^7	8.01×10^5
CTCO2-2	29/12/2011	500.61	1.28×10^5	2.66×10^4
CTCO2-3	04/01/2012	644.61	1.30×10^5	2.76×10^4
CTCO2-4	10/01/2012	788.28	1.13×10^4	6.06×10^3
CTCO2-5	17/01/2012	960.78	4.89×10^5	4.01×10^5
Inoculation fluid	18/01/2012	981.9	5.68×10^5	3.04×10^4
CTCO2-6	24/01/2012	1125.11	2.26×10^4	8.77×10^3
CTCO2-7	31/01/2012	1292.28	7.90×10^4	2.67×10^4
CTCO2-8	07/02/2012	1462.03	1.92×10^5	5.17×10^4
CTCO2-9	14/02/2012	1630.03	1.20×10^5	4.13×10^4
CTCO2-10	21/02/2012	1797.53	7.97×10^4	1.59×10^4
CTCO2-11	28/02/2012	1965.28	3.55×10^6	2.46×10^6
CTCO2-12	06/03/2012	2132.28	3.57×10^5	2.39×10^5

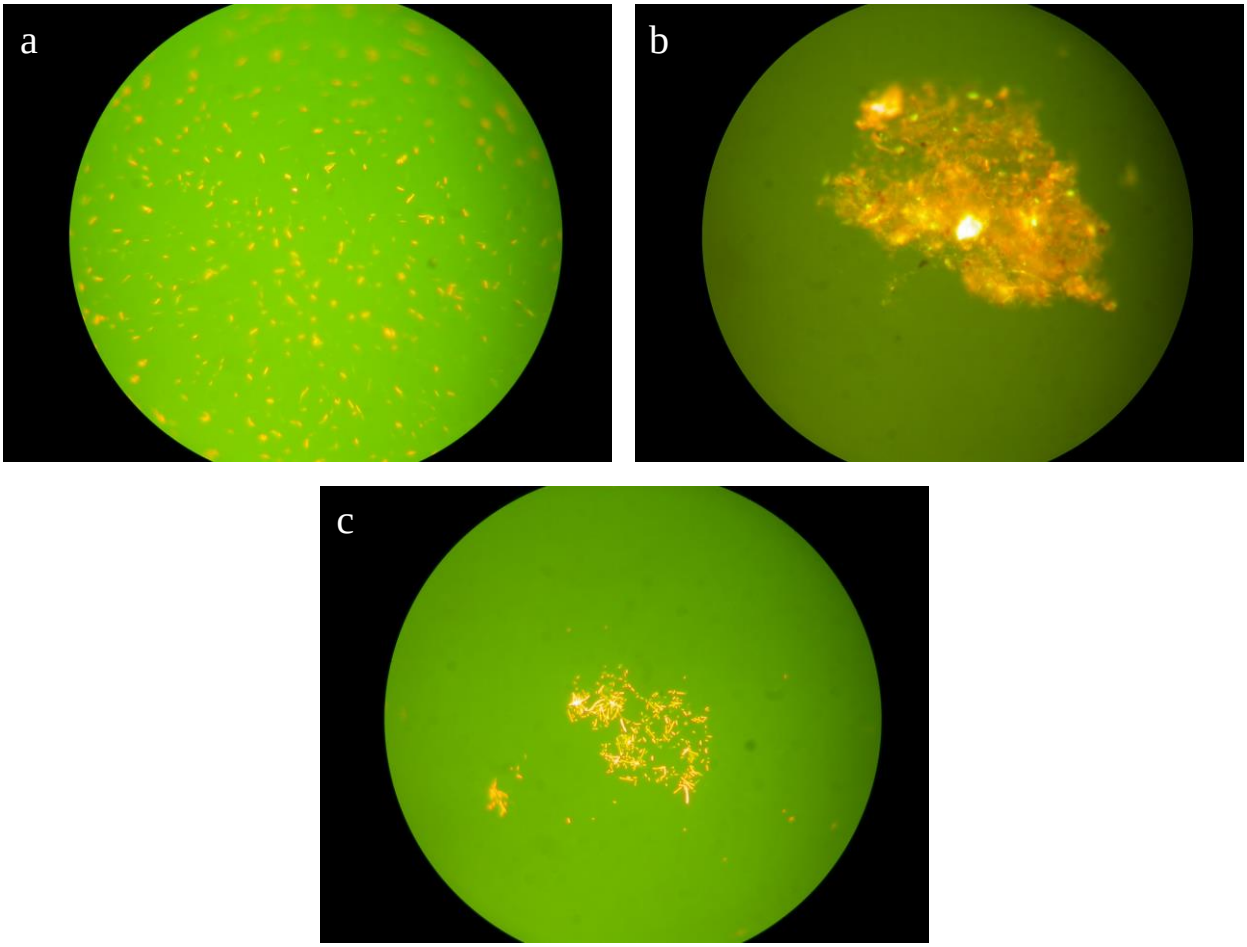

Plate 28 Epifluorescence photographs showing the microbes observed in biotic samples CTCO2-1 (a), CTCO2-9 (b) and CTCO2-11 (c)

4.5 PHYSICAL MEASUREMENT RESULTS

Both control and biotic experiments were performed at a constant flow rate, changes in injection and confining pressure were continuously logged by pressure transducers. An overlay of the biotic and control pressure graphs from the start of the experiment to 2200 h is given in Figure 16.

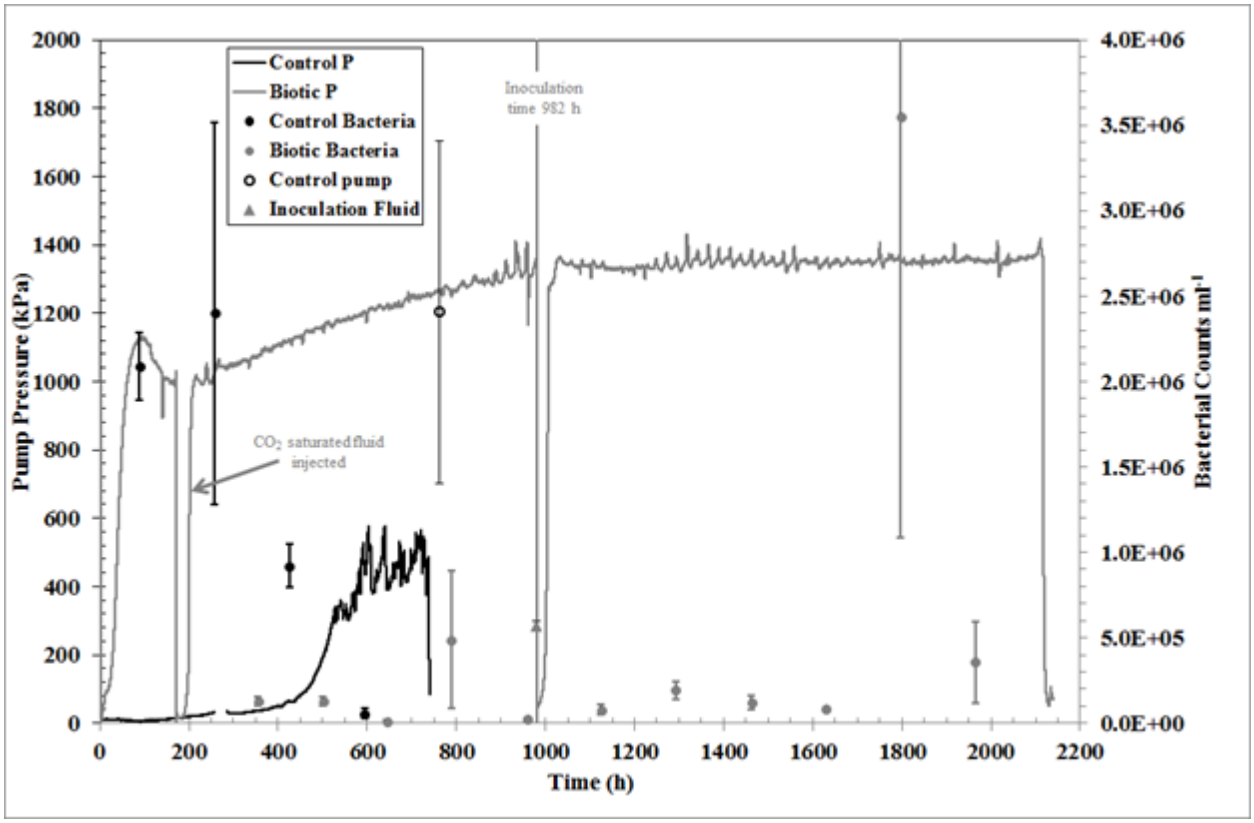

Figure 5 Overlay of recorded pressure and microbial counts in the outflow fluids from the control and biotic columns from the start of each experiment. Black lines and closed circles relate to the control experiment and grey lines and closed circles the biotic experiment. The number of microbes in the inoculant, for the biotic experiment, is denoted by a closed grey triangle. The time of inclusion of saturated CO_2 fluid inoculation are marked on plot.

Figure 5 shows that for the control experiment the presence of backpressure was not evident until 400 h, at which point an increase was observed, reaching 400 – 600 kPa. This range of pressure was observed until termination of the control experiment and though to be associated with biological contamination of the sample, as although microbes were not injected into the system analysis of the outflow fluids indicates their presence after 100 h.

For the biotic core, Figure 5 shows an initial rapid increase in pressure up to *circa.* 1000 kPa, showing a distinct difference compared to the control core. This indicates a difference in the physical properties *e.g.* the heterogeneity of the two materials, although they were collected from side by side in the same original core material. The pressure in the biotic core steadily increases after the inclusion of CO_2 to the saline at 120 h to *ca*. 980 h, where the microbes were added. Beyond this point, the pressure, apart from minor variations, is effectively constant.

4.6 FLUID CHEMISTRY

The results of the fluid chemistry analysis for the control and biotic cores are tabulated in Appendices 2 and 3 respectively. Where data is reported as less than the limit of detection

(LOD), the LOD is set at 0.5 multiplied by the analyte detection limit. Analyses for a number of analytes at the start of the control experiment appear to be spurious.

4.6.1 pH and alkalinity (HCO_3^-)

The pH measurements made on the control and biotic samples collected on removal from the BFA are summarised in Tables 6 and 7 respectively and represented graphically in Figure 4. Table 6 and Figure 4 show that the control pH ranged between 7.3 and 8.1 across the length of the experiment, with a mean pH of 7.7. The mean pH observed for the biotic column experiment was 7.3, lower than that observed for the control column, with a range of 7.0 – 8.1. Figure 4 indicates that for both the control and biotic columns, no correlation between pH and microbial counts was evident. The observed increase in pH up to *ca*. 700 h, in both experiments, compared to the starting fluid, indicates that the pH in both systems is buffered by the rock itself. After this period, in the biotic experiments, the fluid pH drops to *ca*. 7.0, which is higher than expected given the use of a CO_2 rich fluid. This also indicates that the rock itself is buffering any changes in pH. Figure 6 shows the changes in alkalinity, as HCO_3^-, in both the control and biotic experiments and the data is reported in Appendices 2 and 3. As the synthetic groundwater used in the experiment was a solution of NaCl supplemented with sodium acetate, the presence of HCO_3^- ions at a significant concentration would not be expected in the outflow fluids from the control column, which is evidenced by Figure 5. After saturation of the groundwater with CO_2, Figure 6 shows an increase of HCO_3^- ions at ca. 200 h to a relatively constant concentration of *ca*. 650 mg l^{-1} throughout the remainder of the experiment, indicating that the CO_2 containing fluid remains stable with respect to CO_2 concentration.

Table 6 pH measurements for control samples

Sample Name	Sampling Date	Total Time (h)	pH
CT1	08/11/2011 10:00	89.33	7.3
CT2	15/11/2011 10:00	257.33	8.1
CT3	22/11/2011 10:30	425.83	7.5
CT4	29/11/2011 11:00	594.33	7.9
CT5	05/12/2011 10:00	737.33	7.8

Table 7 pH measurements for biotic samples

Sample Name	Sampling Date	Total Time (h)	pH
CTCO2-1	23/12/2011	354.94	7.5
CTCO2-2	29/12/2011	500.61	7.4
CTCO2-3	04/01/2012	644.61	7.3
CTCO2-4	10/01/2012	788.28	7.3
CTCO2-5	17/01/2012	960.78	7.2
CTCO2-6	24/01/2012	1125.11	7.0
CTCO2-7	31/01/2012	1292.28	7.0
CTCO2-8	07/02/2012	1462.03	7.5
CTCO2-9	14/02/2012	1630.03	7.0
CTCO2-10	21/02/2012	1797.53	7.1
CTCO2-11	28/02/2012	1965.28	7.3
CTCO2-12	06/03/2012	2132.28	7.7

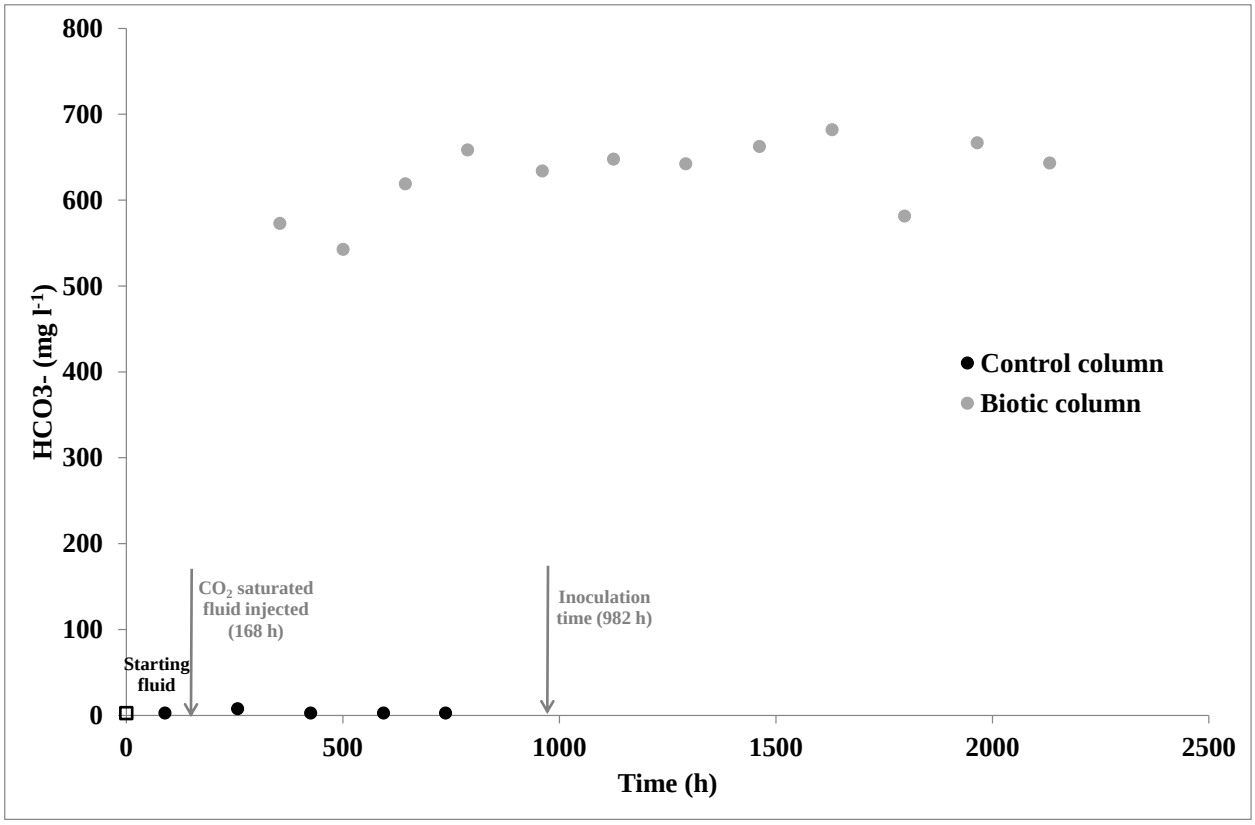

Figure 6 Alkalinity data measured as HCO_3^- for the control and biotic experiments. Closed black and grey circles represent the control and biotic experiments respectively. The HCO_3^- concentration in both starting fluids is shown by an open black square.

4.6.2 Sodium (Na) and Chloride (Cl)

Figures 7 and 8 show the Na and Cl concentrations in the output fluids from both the biotic and control experiments remain constant. This indicates that the major composition of the synthetic groundwater is not influenced by the presence of CO_2, the host rock core or the presence of micro-organisms.

4.6.3 Non Purgeable Organic Carbon (NPOC)

Figure 9 summarises the NPOC data for both columns and shows that the inoculation of organisms at 982 h results in an increase in the amount of soluble organic carbon.

4.6.4 Iron (Fe)

Figure 10 summarise the total Fe concentrations eluting from both columns. The data indicate that both the presence of CO_2 and microbes have little or no influence on the solubility of total Fe in this system. Reduced Fe (Appendices 2 and 3) is below the limit of detection.

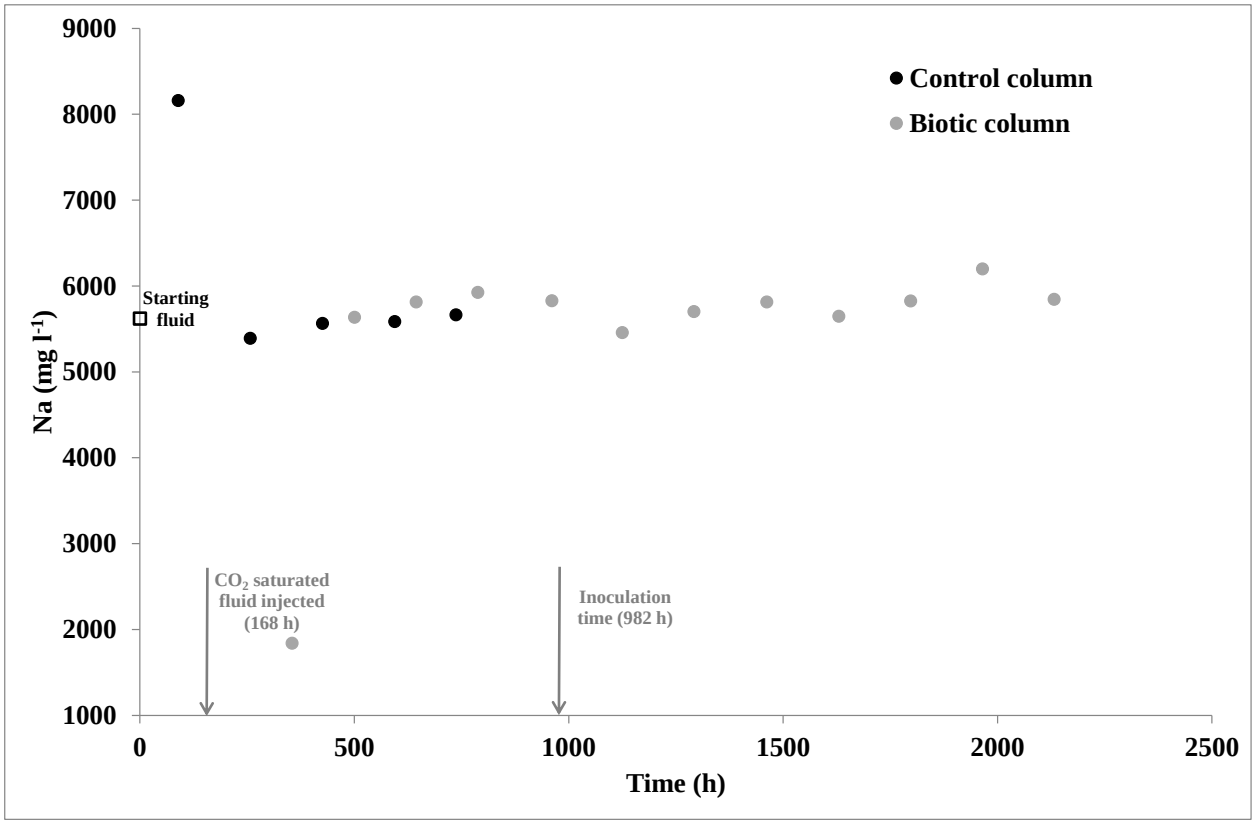

Figure 7 Sodium data for the control and biotic experiments. Closed black and grey circles represent the control and biotic experiments respectively. The sodium concentration in both starting fluids is shown by an open black square.

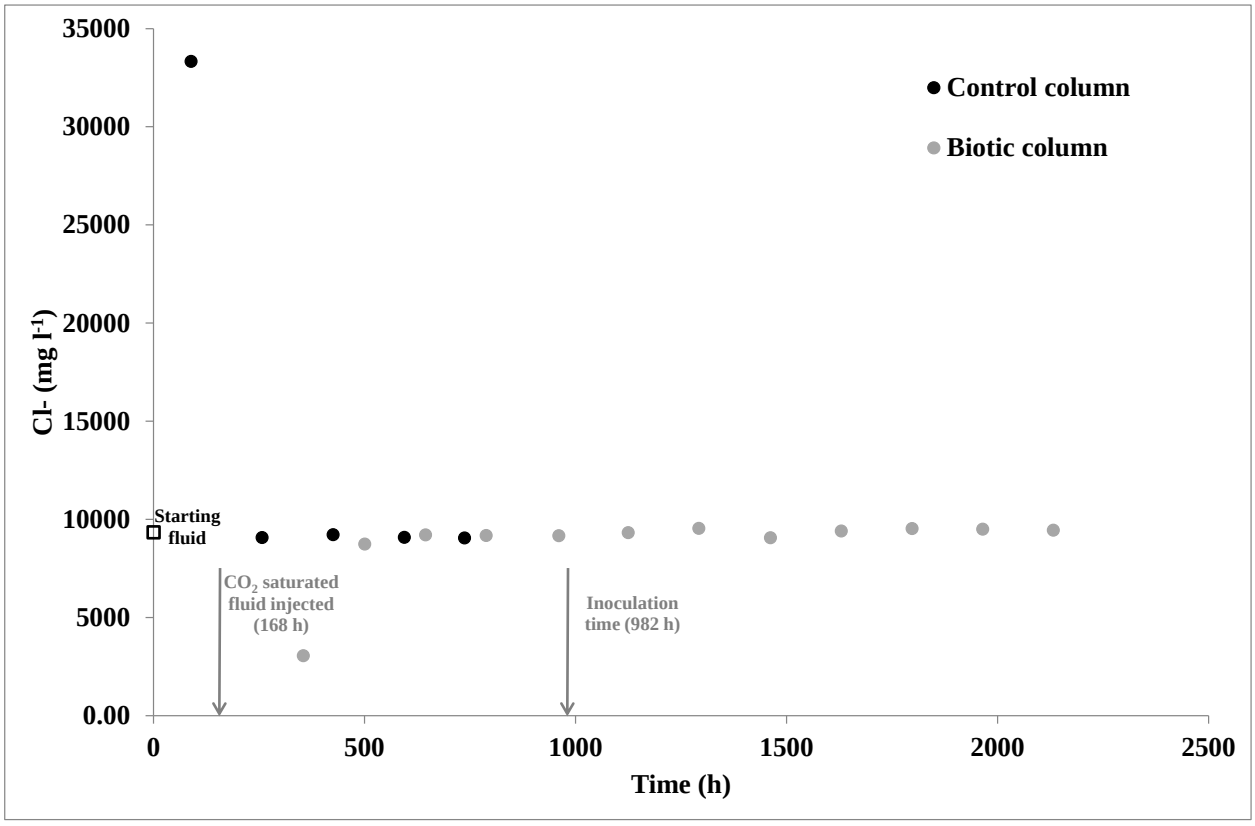

Figure 8 Chloride data for the control and biotic experiments. Closed black and grey circles represent the control and biotic experiments respectively. The chloride concentration in both starting fluids is shown by an open black square.

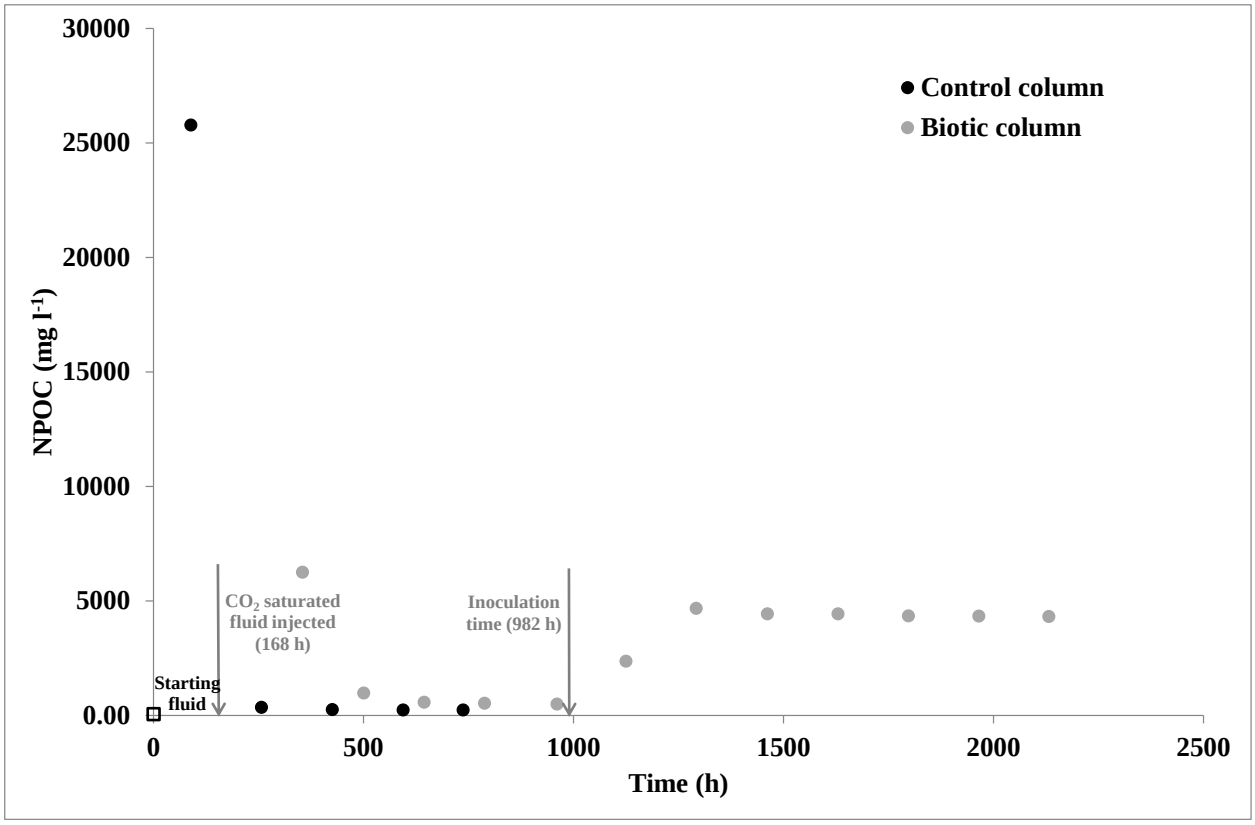

Figure 9 NPOC data for the control and biotic experiments. Closed black and grey circles represent the control and biotic experiments respectively. The NPOC concentration in both starting fluids is shown by an open black square.

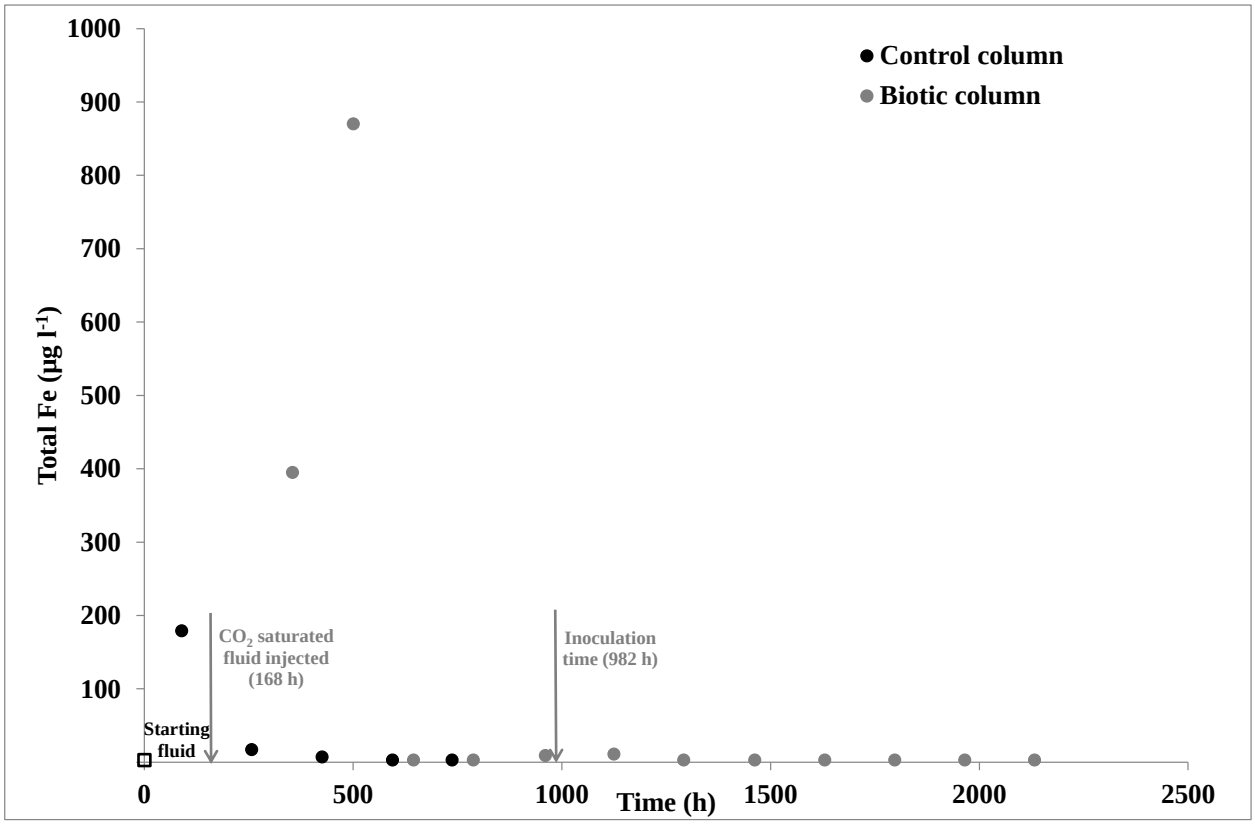

Figure 10 Total iron data for the control and biotic experiments. Closed black and grey circles represent the control and biotic experiments respectively. The iron concentration in both starting fluids is shown by an open black square.

4.6.5 Magnesium (Mg) and Nickel (Ni)

Figures 11 and 12 demonstrate that when CO_2 is introduced into the fluids the release of Mg and Ni is enhanced. The release of Ni may be a result of partial dissolution of the piping used in the BFA, as Ni is a component of steel; however this is unlikely because of the pH observed in the outflow fluids (Figure 4) is not acidic. The presence of Ni is more likely to be associated with the chlorite in the host rock material. The source of the Mg is most likely to be dolomite and/or chlorite, both Mg rich minerals identified as present in the post experiment host rock material (Table 2), which would dissolve in the presence of CO_2.

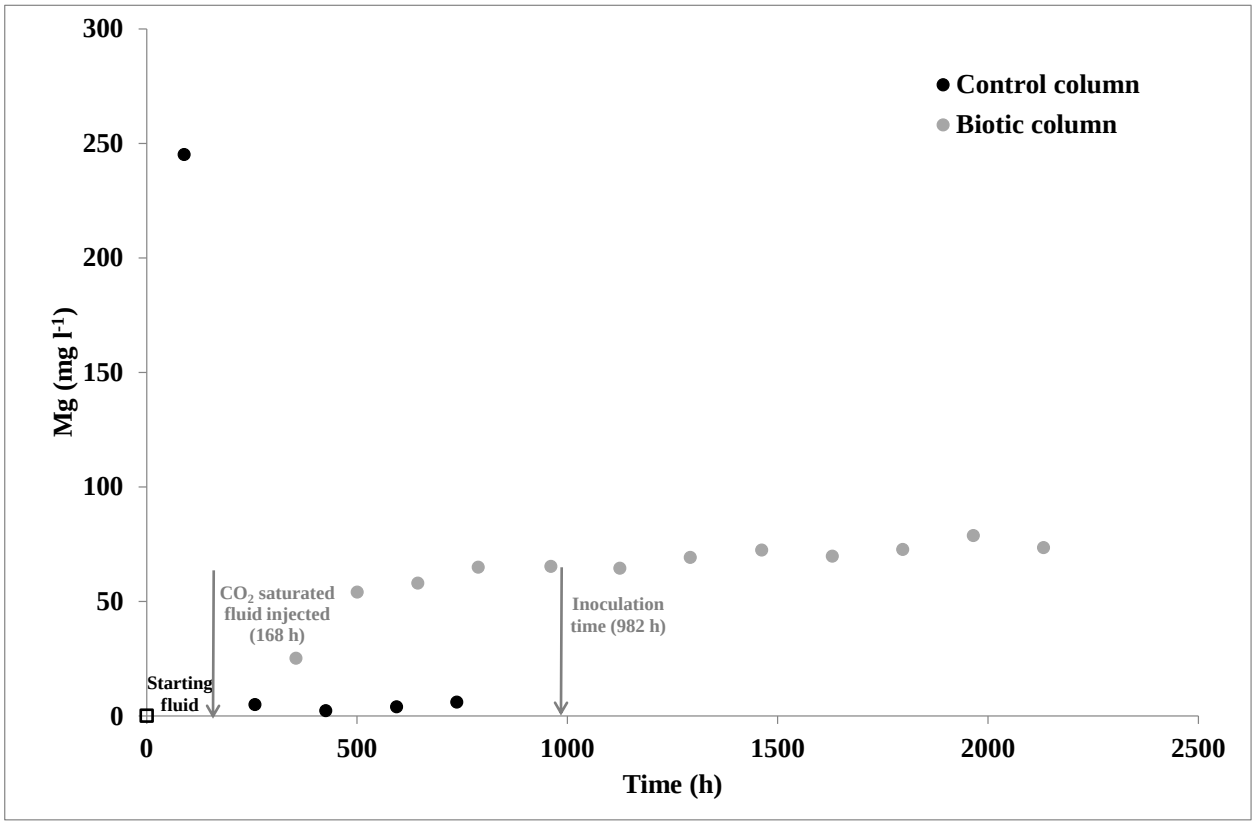

Figure 11 Magnesium data for the control and biotic experiments. Closed black and grey circles represent the control and biotic experiments respectively. The magnesium concentration in both starting fluids is shown by an open black square.

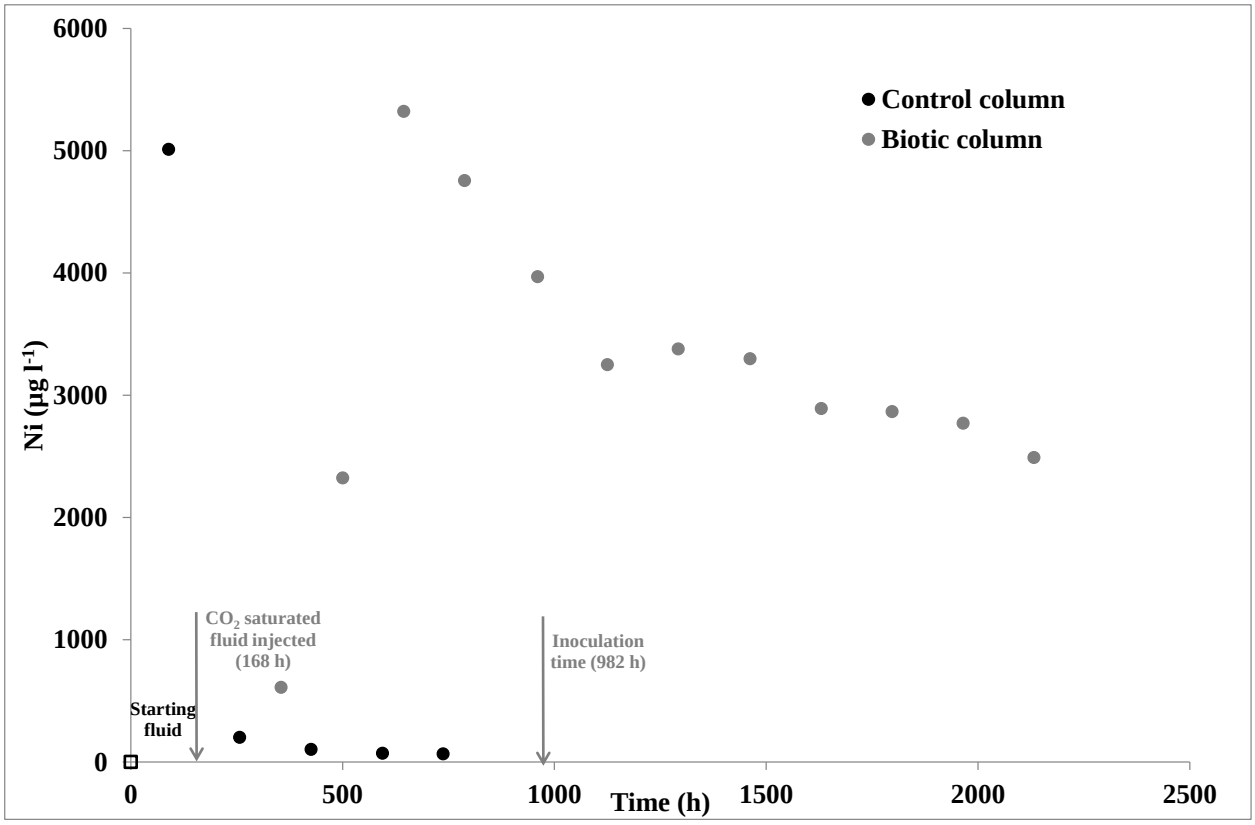

Figure 12 Nickel data for the control and biotic experiments. Closed black and grey circles represent the control and biotic experiments respectively. The nickel concentration in both starting fluids is shown by an open black square.

4.6.6 Potassium (K), Silicon (Si) and Antimony (Sb)

Figures 13 - 15 summarise the Si, K and Sb data for the two experiments. Figure 13 shows similar trends for both experiments, where between *ca*. 250 and 600 h a peak is observed relating to the release of *ca.* 300-500 mg l^{-1} K. Chlorite, micas and k-feldspar are potential sources of the leachable K (Table 2). A similar trend is seen in Figure 15 for Sb, where *ca*. 2 ug l^{-1} is released over a slightly longer timescale (up to 1000 h). This is thought to be associated with the mobilisation of clay fines and the associated trace elements. It is also likely that Si associated with clay coatings is mobilised during both experiments (Figure 14). However, Figure 14 indicates that the release of Si is enhanced in the biotic experiment when compared to the control.

4.6.7 Tungsten

Figure 16 shows the release of W in both experiments over time. Peaks early (*ca.* 300 h) in both the control and biotic experiments suggest the presence of relatively mobile W. A possible source of W is the W-carbide cutting blade, used to prepare the core materials.

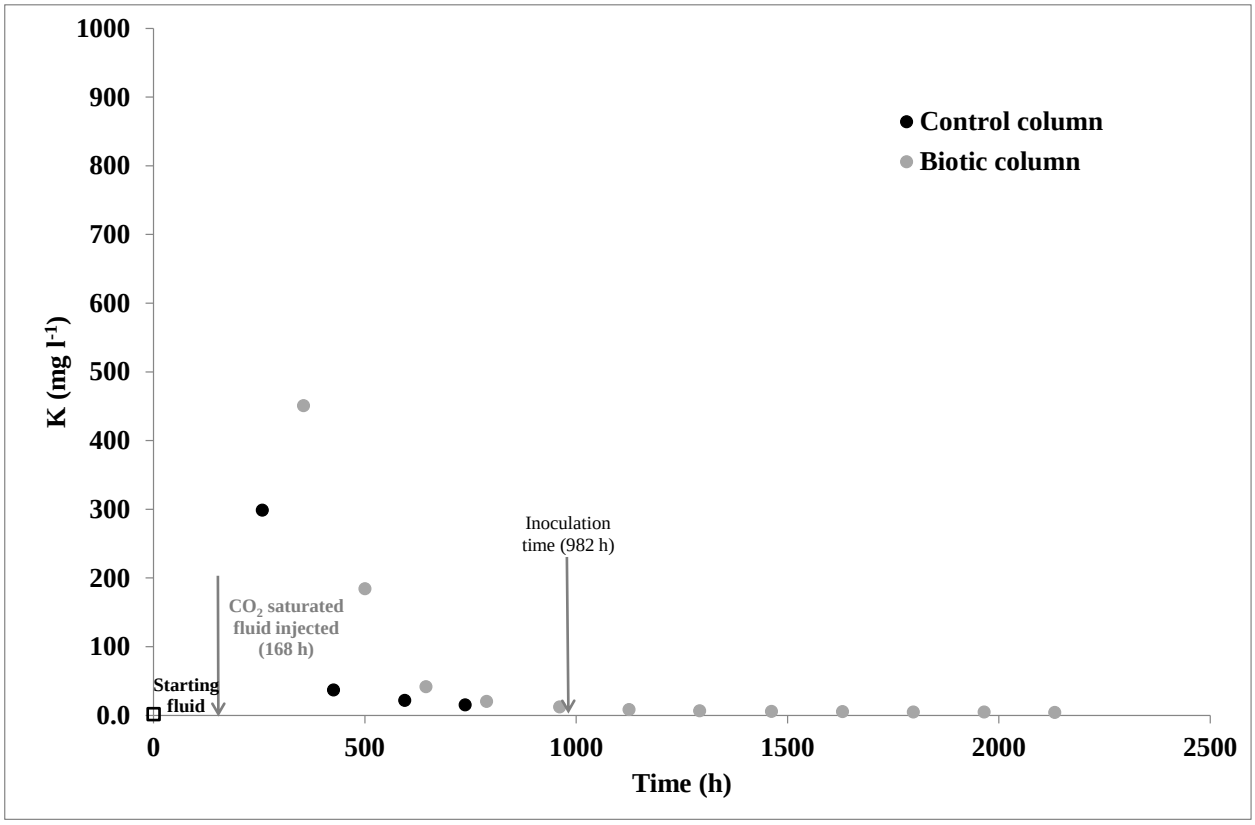

Figure 13 Potassium data for the control and biotic experiments. Closed black and grey circles represent the control and biotic experiments respectively. The potassium concentration in both starting fluids is shown by an open black square.

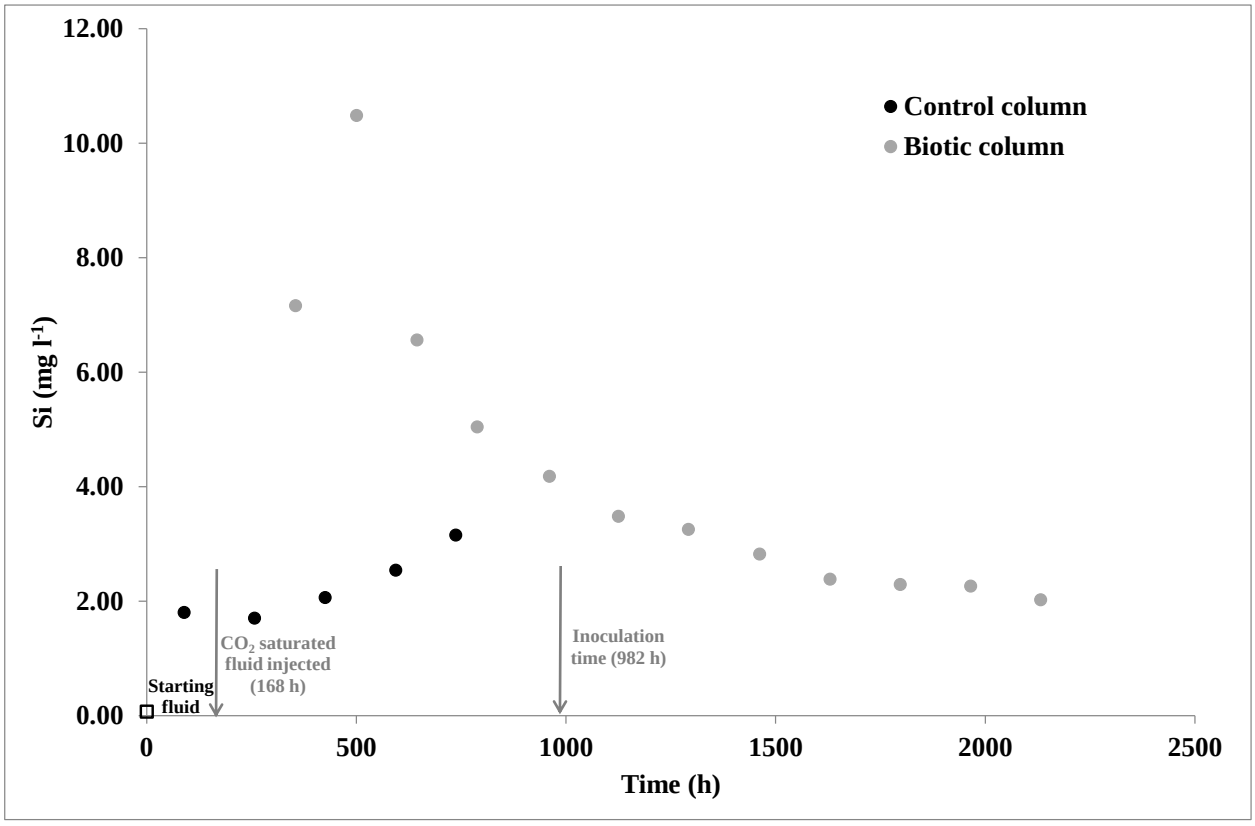

Figure 14 Silicon data for the control and biotic experiments. Closed black and grey circles represent the control and biotic experiments respectively. The silicon concentration in both starting fluids is shown by an open black square.

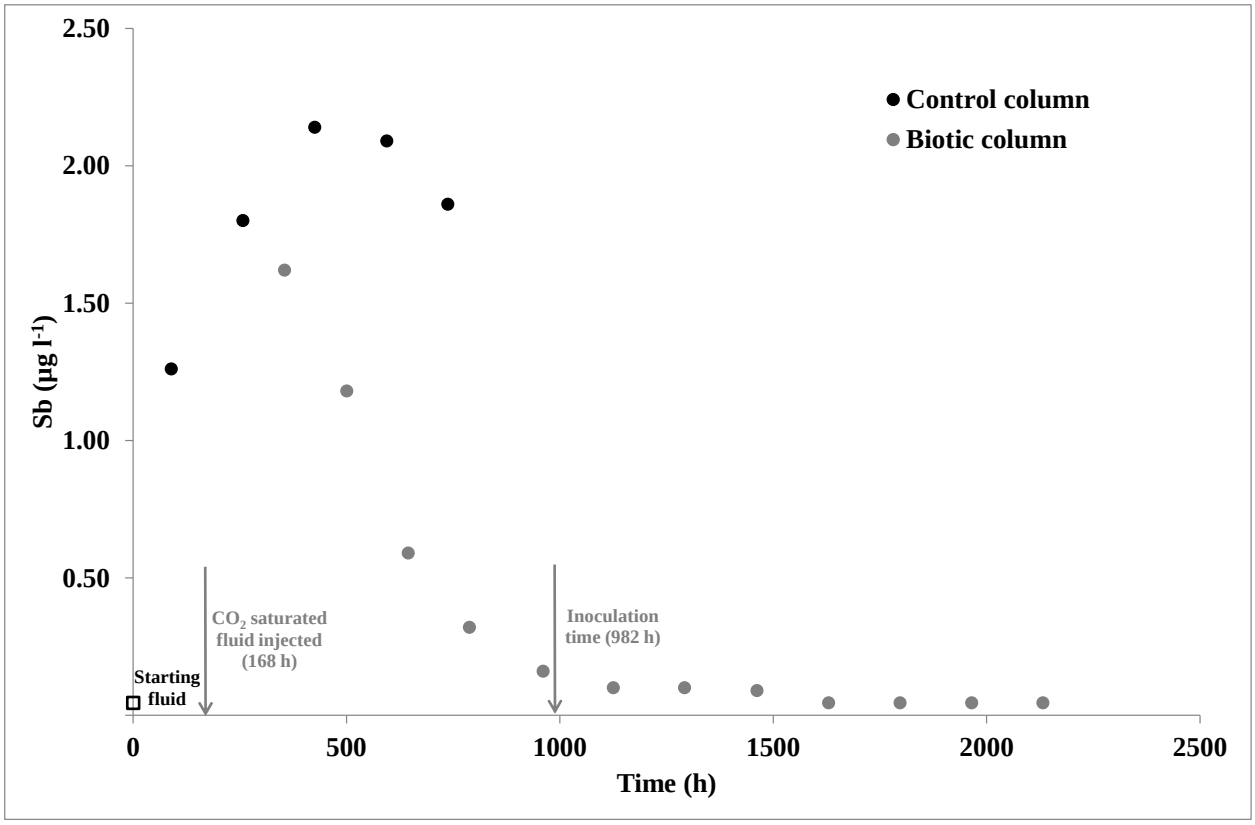

Figure 15 Antimony data for the control and biotic experiments. Closed black and grey circles represent the control and biotic experiments respectively. The antimony concentration in both starting fluids is shown by an open black square.

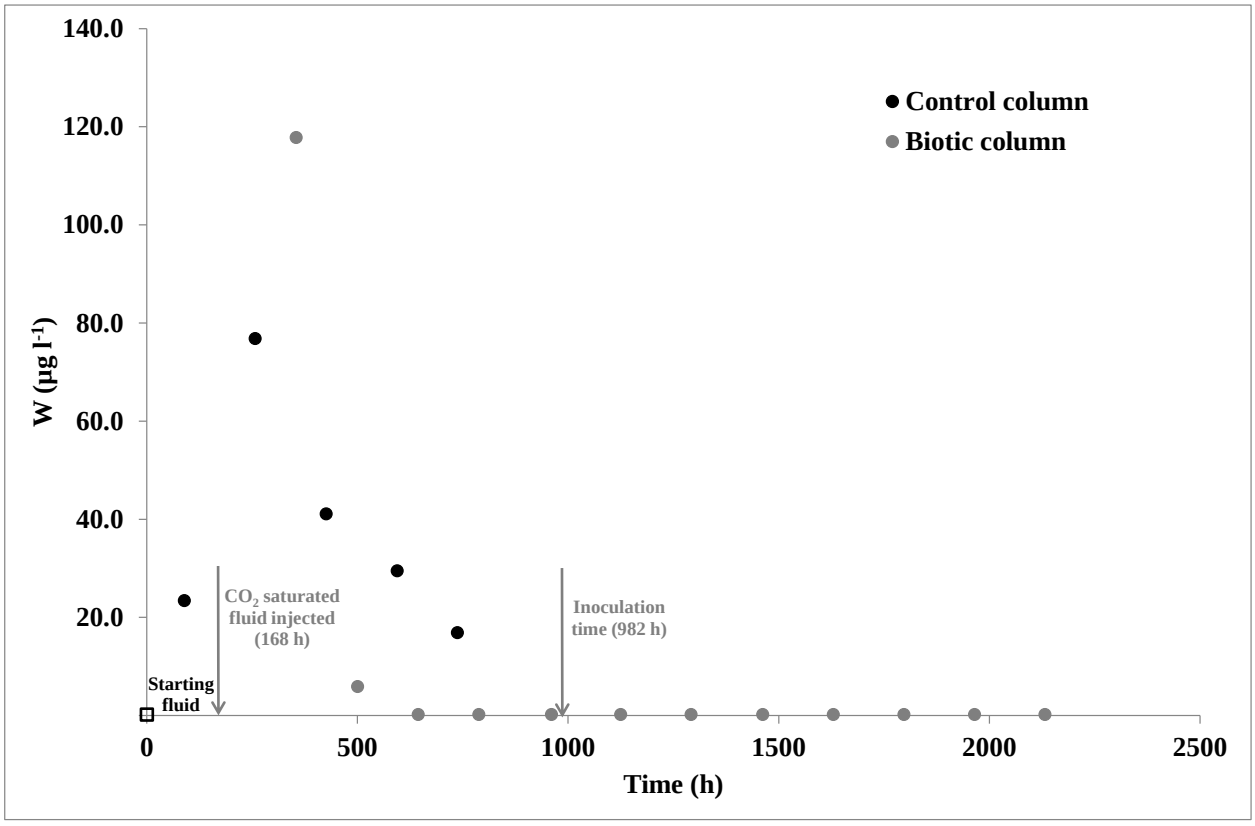

Figure 16 Tungsten data for the control and biotic experiments. Closed black and grey circles represent the control and biotic experiments respectively. The tungsten concentration in both starting fluids is shown by an open black square.

5 Discussion

5.1 WHOLE ROCK AND CLAY MINERALOGY

Comparison of XRD analysis of both post-test materials indicates that no significant differences were apparent between the control and biotic residues. However, analysis of clay mineralogy data for the control and biotic residues indicated trace amounts of smectite (estimated <1% of the clay fraction) to be associated with the biotic column. This observation may be the result of the introduction of microbes into the biotic column or as a result of sample heterogeneity (*e.g.* laminations within the sandstone).

5.2 PETROGRAPHY

5.2.1 Control Sample

A pore lining of a film-like phase was observed at the inlet end and within the sample material. This film-like phase was noted to be more common at the inlet end. Some of the characteristics of the film-like phase are consistent with it being a biofilm. These include its general appearance, a tendency to be associated with fines and sensitivity to the electron beam. There are also rare cell-like forms on pore walls that are of the correct size (< 2 µm) to be of microbial origin.

These observations are consistent with the sample having been microbially colonised at some point during the experiment.

The fibrous phase noted within some patches of the film could be a constituent of the film or illitic clay. Fibrous illitic clay is a diagenetic constituent of the rock and could have been detached and entrained in the flow of test liquid, then subsequently trapped in the film.

5.2.2 Biotic Sample

A pore lining of a film-like phase was observed throughout the post-test biotic sample material, with considerably greater abundance at the inlet end and central plug portions than at the outlet end. Some of the characteristics of the film-like phase are consistent with it being a biofilm. These include its general appearance, a tendency to be associated with fines and sensitivity to the electron beam. There are also widespread cell-like forms associated with some patches of film that are of the correct size (< 3 µm) to be microbial.

These observations are consistent with the sample having been microbially colonised. The development of biofilm and evidence of microbial cells is significantly greater than that observed in the control sample.

At some sites where pore walls extend towards the centres of pores, film and associated fines are more abundant. This suggests that colonisation may be favoured at sites exposed to more rapidly moving nutrient-bearing test fluids.

A localised fibrous phase noted associated with some patches of the film is most likely of illitic clay, as at some sites their morphology is well displayed. In some cases these appear to be grain-coating clay constituents that have collapsed in situ, in others the fibres are detached, suggesting they have become mobilised before being trapped by the film. Examples of collapsed illitic fibres identified in the absence of the probable biofilm, show that collapse is not necessarily related to the presence or formation of the film; collapse may have occurred before, during or after the testing.

5.2.3 Grey Staining

A deposit of a non-aqueous droplet like phase was observed only on the surface of the material, where the grey stain was observed. No other phases were observed in the area. It is not possible to know for certain if the droplets are responsible for or related to the grey colour. However, no

other additional phase was observed in the sample portion analysed. No similar droplets were observed in any other portion of the sample. This material may be oil contamination, from greases used on the pressure fittings of the apparatus, which has been transferred to the core, possibly as a result of a small imperfection or hole in the heat shrunk PTFE sheath which may represent and additional microbial food source.

5.3 MICROBIOLOGICAL AND PHYSICAL MEASUREMENTS

Changes in physical pressure measurement (injection and confining pressure) were continuously monitored with injection pressure presented in Figure 5 together with microbial numbers for both control and biotic experiments. For the biotic core, Figure 5 shows an initial rapid increase in pressure up to circa. 1000 kPa, showing a distinct difference compared to the control core. After the injection of the CO_2 saline solution, the pressure in the biotic core steadily increases from 120 h (5 days), to *ca*. 980 h (41 days). Beyond this time, and after the injection of *P. aeruginosa*, the pressure, apart from minor variations, is effectively constant. Figure 5 shows that, for the control experiment, there was no backpressure until 400 h. At this point, an increase in pressure was observed, reaching 400 – 600 kPa between 550 and 700 h.

The differences in pressure in the biotic and control experiments suggest a difference in flow characteristics and physical properties in the two samples although they were sampled from the same depth in the original core material. Both of the plugs used in this study comprise fine to medium grained sandstones that have finely defined laminar bedding planes. These are shown as fine variations in colour in Plate 5. The thin darker laminations are sediment intervals that have higher detrital clay content. The distribution of these laminations represent a potential source of heterogeneity between samples even when they have been taken from horizontally adjacent sites, as the laminations are inclined. Indeed, the biotic plug sample was noted to have a high concentration of the clay-rich laminations at its inlet end (note the overall darker red colour at the top of Plate 16); this concentration was not observed in the control plug sample.

These results demonstrate that in this short study, the injection of *P. aeruginosa* into the biotic experiment does not appear to impact on the physical transport properties of the Sherwood Sandstone. However, in other work which utilised the same organism and rock type but with no introduction of CO_2 saturated fluid, post-inoculation injection changes were observed. These included short but rapid saw-tooth like changes in the pressure profile (Wragg et al, 2012). These impacts were not observed in the current study which suggests that the CO_2 saturated fluid was reducing the tendency for the microbes to alter permeability.

After CO_2 injection, microbial numbers in the biotic experiment rapidly drop from ~$1.16x10^7$ ml^{-1} (SE $8.01x10^5$ ml-1) at 354 hours to approximately 10^5 organism's ml^{-1} at the end of the experiment (Figure 5). In the control experiment, numbers in the outflow fluids drop from approximately $2.0x10^6$ (SE 10^4 ml^{-1}) to approximately $2.6x10^4$ ml^{-1} (SE $3x10^4$ ml^{-1}) at the end of the experiment. Thus, an indigenous population is present in the host rock. Other work (Harrison et al, 2011) has shown that such populations can impact on fluid transport in rocks because of the formation of biofilms that then impact on rock transport properties. In this study, such a build-up of pressure does not appear to occur in the biotic experiment where indigenous populations and injected *P. aeruginosa* appear to be impacted by the presence of CO_2. However, a microbial population still exists in the biotic experiments demonstrating that, despite the extreme environmental conditions generated by the presence of CO_2, microorganisms are able to survive. It is possible that the impacts of these microbes on fluid flow will take longer to observe because a period of acclimatisation may be necessary. Consequently, it is important to carry out longer term experiments in order to determine the significance of microbial activity on transport of CO_2 in host rocks relevant to carbon capture and storage.

The microbial biomass counts for the control experiment highlight the presence of indigenous species in this test system and the presence of acetate in the saline groundwater will have stimulated growth. However, acetate was only added to the saline groundwater to allow for

direct comparison with the 'biotic' experiment. Injection of contaminated groundwater could be one explanation for the high microbial count in the 'control' experiment, but microbes were not detected in the starting fluid, suggesting this is not the source of the microbes.

5.4 CHEMICAL MEASUREMENTS

Migration of chemical species through and from the host rock core under control and biotic conditions was monitored over the lifetime of the experiments and selected elemental data summarised in Figures 5 – 15. Figures 5 – 7 show that the chemistry of the system is relatively constant, i.e. Cl and Na and, when introduced into the system HCO_3.. In general the data suggest that the presence of CO_2, rather than the microbes, enhances the release and subsequent migration of elements associated with the host rock in the experiments in this study (Figures 10 – 15).

6 Conclusion and recommendations

The effect of CO_2 on the activity of any indigenous or introduced microbial populations and resulting impacts on a storage facility, including the movement of the CO_2 plume, is an area of uncertainty. It is likely that impacts may only apply to storage schemes in specific geological settings (West et al, 2011). Given these uncertainties, the precautionary principle suggests that the potential impacts should be quantified before projects are initiated. This pilot study is the first to investigate the changes in physical transport properties that are mediated by microbial activity within sandstone samples, under experimental conditions, simulating CO_2 saturated fluid movement in deep aquifer and reservoir environments in the North Sea. These short experiments utilised *P. aeruginosa* and indigenous microbial populations and showed, for the first time, that these organisms can survive exposure to saline fluids saturated with CO_2 albeit with limited biofilm development.

The impacts of CO_2 in the test system are twofold:

- The organisms do not seem to inhibit fluid transport under these conditions in these short experiments (2136 h/ 89 days). It is possible that the microbes require a period of acclimatisation to the extreme environmental conditions generated by the presence of CO_2 before any impacts can be detected;
- The presence of CO_2 appears to enhance the mobilisation of a number of chemical species.

Longer term experiments are considered necessary to determine whether the presence of CO_2 merely delays biofilm development and/or impacts on permeability or whether it causes long-term inhibition of microbial activity. Additionally, the role of impurities (such as H_2S, SO_X and NO_X) that may be present in the injected CO_2 could be involved in microbial energy production (West *et al*, 2011) and also needs to be studied. Thus, long-term experiments are needed to clarify the role of microbes on rock transport properties.

This initial study has also identified specific areas for further study, these are:

- Undertaking a double control experiment, where no acetate is added to the simulated groundwater, thus denying food and energy to any native microbes, and;
- Undertaking a simplified experiment using the pump set-up alone to determine whether the cleaning/sterilisation process in current use is fit for purpose.

Appendix 1 X-ray Diffraction Traces

KEY

Vertical axis – Intensity (counts per second)

Horizontal axis - °2θ Co-Kα

For the <2 µm trace, the black trace (air-dry), red trace (glycol-solvated), green trace (heated 550°C/2 hours). Only the most intense/diagnostic peak of each identified mineral is labelled with its corresponding d(Å) spacing.

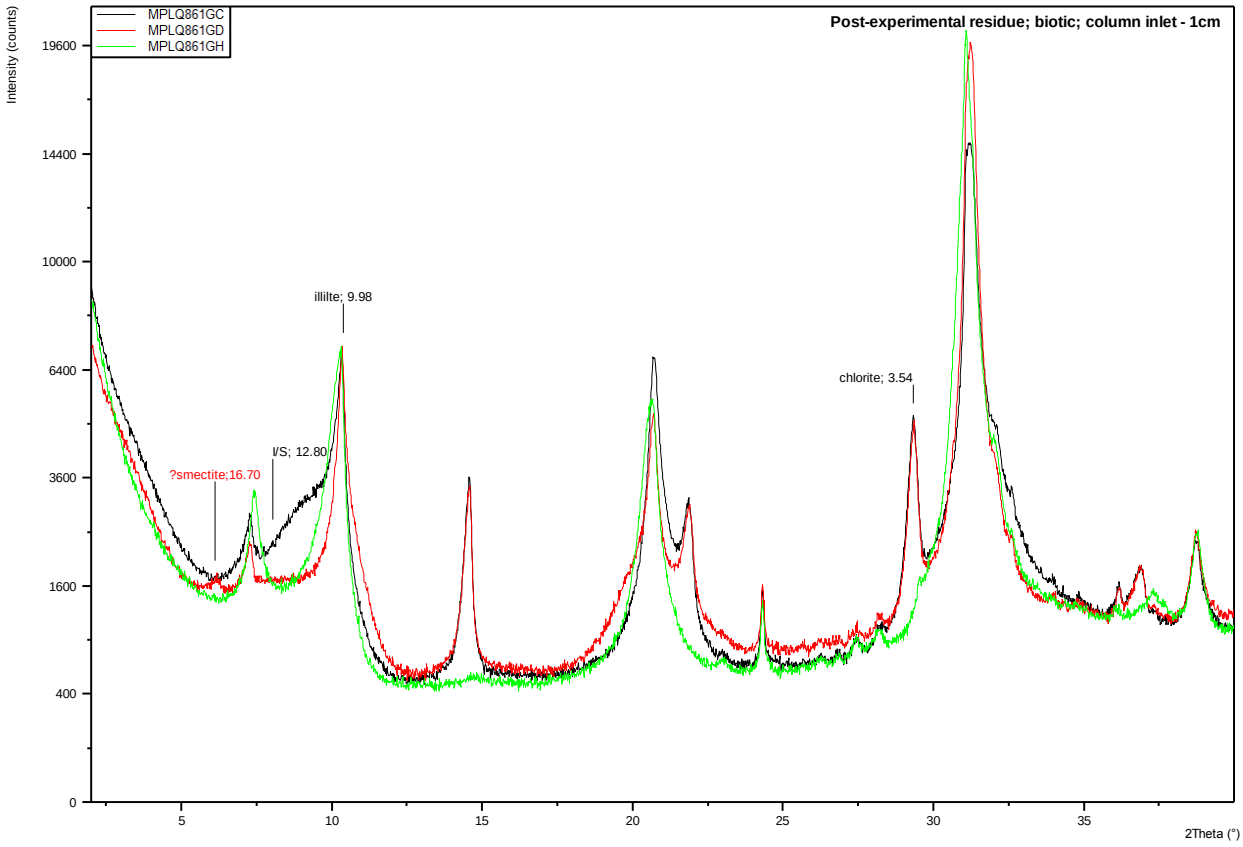

Appendix 2 Chemistry data for the control column

Sample	Sample description	Total time	pH	Ca	Mg	Na	K	HCO_3^-	Cl^-	SO_4^{2-}	NO_3^-	Br^-	NO_2^-	HPO_4^{2-}	F^-	I	NPOC
				mg l^{-1}	mg l^{-1}	mg l^{-1}	mg l^{-1}	mg l^{-1}	mg l^{-1}	mg l^{-1}	mg l^{-1}	mg l^{-1}	mg l^{-1}	mg l^{-1}	mg l^{-1}	µg l^{-1}	mg l^{-1}
CT1	Sampled fluid ex core	89	7.33	171	245	8159	18018	2.50	33330	427	137	50.1	2.50	25.0	2.50	40.8	25775
CT2	Sampled fluid ex core	257	8.08	19	4.9	5390	299	7.5	9062	12.5	5.0	5.0	2.50	25.0	2.50	2.0	348
CT3	Sampled fluid ex core	426	7.47	15	2.2	5563	36.7	2.50	9208	12.5	5.0	5.0	2.50	25.0	2.50	1.0	247
CT4	Sampled fluid ex core	594	7.87	18	3.9	5585	21.6	2.50	9076	12.5	10.1	5.0	2.50	25.0	2.50	0.9	232
CT5	Sampled fluid ex core	737	7.79	26	6.0	5664	15.1	2.50	9048	12.5	5.0	5.0	2.50	25.0	2.50	0.8	227
Starting fluid		0	6.48	1	0.1	5621	1.8	2.50	9341	12.5	32.1	5.0	2.50	25.0	2.50	0.1	50
Fluid in pump at experiment end		761	7.71														

Sample	Sample description	Total time	Total P	Total S	Si	SiO_2	Ba	Sr	Mn	Total Fe	Fe (II)	Li	Be	B	Al	Ti	V
			mg l^{-1}	mg l^{-1}	mg l^{-1}	mg l^{-1}	µg l^{-1}	µg l^{-1}	µg l^{-1}	µg l^{-1}	µg l^{-1}	µg l^{-1}	µg l^{-1}	µg l^{-1}	µg l^{-1}	µg l^{-1}	µg l^{-1}
CT1	Sampled fluid ex core	89	0.22	231	1.80	3.85	223	2109	1268	179	n/s	1121	0.02	130	5	1.0	2
CT2	Sampled fluid ex core	257	0.04	9	1.70	3.64	121	211	62	17	37.5	33	0.02	130	5	0.3	13
CT3	Sampled fluid ex core	426	0.04	5	2.06	4.41	92	132	46	7	37.5	16	0.02	130	5	0.3	2
CT4	Sampled fluid ex core	594	0.04	5	2.54	5.43	107	119	44	3	37.5	14	0.02	130	5	0.3	3
CT5	Sampled fluid ex core	737	0.11	5	3.15	6.74	140	129	59	3	37.5	6	0.02	130	13	0.3	2
Starting fluid		0	0.04	5	0.07	0.150	1	2	1	3	n/s	6	0.02	130	5	0.3	2

Sample	Sample description	Total time	Cr	Co	Ni	Cu	Zn	Ga	As	Se	Rb	Y	Zr	Nb	Mo	Ag	Cd
			µg l^{-1}	µg l^{-1}	µg l^{-1}	µg l^{-1}	µg l^{-1}	µg l^{-1}	µg l^{-1}	µg l^{-1}	µg l^{-1}	µg l^{-1}	µg l^{-1}	µg l^{-1}	µg l^{-1}	µg l^{-1}	µg l^{-1}
CT1	Sampled fluid ex core	89	12.5	153	5010	161	112	1	126	27.4	5075	0.05	0.3	0.3	714	21.9	12.5
CT2	Sampled fluid ex core	257	1.7	4.68	201	27.7	17	1	23.7	5.8	163	0.02	0.3	0.3	330	0.17	0.18
CT3	Sampled fluid ex core	426	0.3	2.29	102	10.8	20	1	21.3	3.4	53.8	0.02	0.3	0.3	329	0.04	0.13
CT4	Sampled fluid ex core	594	0.3	1.97	70.0	4.0	14	1	19.5	3.3	37.8	0.02	0.3	0.3	301	0.04	0.17
CT5	Sampled fluid ex core	737	0.3	3.69	66.3	1.9	8	1	14.7	2.8	29.9	0.02	0.3	0.3	209	0.04	0.16
Starting fluid		0	0.3	0.04	0.3	5.2	14	1	14.0	2.9	3.06	0.02	0.3	0.3	1	0.04	0.07

Sample	Sample description	Total time	Sn	Sb	Cs	La	Ce	Pr	Nd	Sm	Eu	Gd	Tb	Dy	Ho	Er	Tm
			µg l^{-1}	µg l^{-1}	µg l^{-1}	µg l^{-1}	µg l^{-1}	µg l^{-1}	µg l^{-1}	µg l^{-1}	µg l^{-1}	µg l^{-1}	µg l^{-1}	µg l^{-1}	µg l^{-1}	µg l^{-1}	µg l^{-1}
CT1	Sampled fluid ex core	89	1.9	1.26	166	0.01	0.02	0.06	1	0.04	0.01	0.013	0.004	0.03	0.004	0.03	0.004
CT2	Sampled fluid ex core	257	0.6	1.80	7.09	0.01	0.02	0.02	1	0.05	0.01	0.004	0.004	0.01	0.004	0.03	0.004
CT3	Sampled fluid ex core	426	0.4	2.14	3.19	0.01	0.02	0.02	1	0.05	0.01	0.004	0.004	0.01	0.004	0.03	0.004
CT4	Sampled fluid ex core	594	0.3	2.09	2.48	0.01	0.02	0.02	1	0.02	0.01	0.004	0.004	0.01	0.004	0.03	0.004
CT5	Sampled fluid ex core	737	0.3	1.86	2.09	0.01	0.02	0.02	1	0.02	0.01	0.004	0.004	0.01	0.004	0.03	0.004
Starting fluid		0	0.1	0.05	0.26	0.01	0.02	0.02	1	0.02	0.01	0.004	0.004	0.01	0.004	0.03	0.004
Fluid in pump at experiment end		761															

Sample	Sample description	Total time	Yb	Lu	Hf	Ta	W	Tl	Pb	Th	U
			µg l^{-1}	µg l^{-1}	µg l^{-1}	µg l^{-1}	µg l^{-1}	µg l^{-1}	µg l^{-1}	µg l^{-1}	µg l^{-1}
CT1	Sampled fluid ex core	89	0.019	0.004	0.4	0.1	23.4	14.9	0.1	0.3	0.66
CT2	Sampled fluid ex core	257	0.004	0.004	0.1	0.1	76.8	0.53	0.1	0.3	0.25
CT3	Sampled fluid ex core	426	0.004	0.004	0.1	0.1	41.1	0.21	0.1	0.3	0.28
CT4	Sampled fluid ex core	594	0.004	0.004	0.1	0.1	29.5	0.13	0.1	0.3	0.54
CT5	Sampled fluid ex core	737	0.004	0.004	0.1	0.1	16.9	0.10	0.1	0.3	0.81
Starting fluid		0	0.004	0.004	0.1	0.1	0.2	0.02	0.1	0.3	0.04
Fluid in pump at experiment end		761									

Appendix 3 Chemistry data for the biotic column

Sample	Sample description	Total time	pH	Ca	Mg	Na	K	HCO_3^-	Cl^-	SO_4^{2-}	NO_3^-	Br^-	NO_2^-	HPO_4^{2-}	F^-	I	NPOC
				mg l^{-1}	mg l^{-1}	mg l^{-1}	mg l^{-1}	mg l^{-1}	mg l^{-1}	mg l^{-1}	mg l^{-1}	mg l^{-1}	mg l^{-1}	mg l^{-1}	mg l^{-1}	µg l^{-1}	mg l^{-1}
CTCO2-1	Fluid ex core	355	7.45	115	25.1	1840	451	573	3046	12.5	19.3	5.0	2.50	25.0	2.50	1.9	6244
CTCO2-2	Fluid ex core	501	7.42	212	54.0	5635	184	543	8739	12.5	11.2	5.0	2.50	25.0	2.50	0.8	970
CTCO2-3	Fluid ex core	645	7.34	123	57.9	5813	41.6	619	9204	12.5	13.0	5.0	2.50	25.0	2.50	0.6	567
CTCO2-4	Fluid ex core	788	7.33	121	64.9	5925	20.3	658	9171	12.5	12.4	5.0	2.50	25.0	2.50	0.4	524
CTCO2-5	Fluid ex core	961	7.18	115	65.2	5828	12.3	634	9157	12.5	16.1	5.0	2.50	25.0	2.50	0.3	493
CTCO2-6	Fluid ex core	1125	7.01	108	64.4	5456	8.20	648	9321	12.5	5.0	5.0	2.50	25.0	2.50	0.5	2364
CTCO2-7	Fluid ex core	1292	7.02	115	69.2	5701	6.50	642	9533	12.5	5.0	5.0	2.50	25.0	2.50	0.5	4674
CTCO2-8	Fluid ex core	1462	7.48	122	72.4	5814	5.70	662	9053	12.5	5.0	5.0	2.50	25.0	2.50	0.5	4430
CTCO2-9	Fluid ex core	1630	7.04	117	69.7	5647	5.30	682	9401	12.5	5.0	5.0	2.50	25.0	2.50	0.5	4426
CTCO2-10	Fluid ex core	1798	7.06	120	72.6	5825	4.90	581	9529	12.5	5.0	5.0	2.50	25.0	2.50	0.5	4340
CTCO2-11	Fluid ex core	1965	7.25	128	78.7	6199	4.80	667	9492	12.5	38.2	5.0	2.50	25.0	2.50	0.5	4330
CTCO2-12	Fluid ex core	2132	7.71	122	73.4	5843	4.10	643	9438	26.8	285	31.4	2.50	25.0	2.50	0.5	4312
Starting fluid		0.0	6.48	1.00	0.1	5621	1.80	2.50	9341	12.5	32.1	5.0	2.50	25.0	2.50	0.1	50.0

Sample	Sample description	Total time	Total P	Total S	Si	SiO_2	Ba	Sr	Mn	Total Fe	Fe (II)	Li	Be	B	Al	Ti	V
			mg l^{-1}	mg l^{-1}	mg l^{-1}	mg l^{-1}	µg l^{-1}	µg l^{-1}	µg l^{-1}	µg l^{-1}	µg l^{-1}	µg l^{-1}	µg l^{-1}	µg l^{-1}	µg l^{-1}	µg l^{-1}	µg l^{-1}
CTCO2-1	Fluid ex core	355	0.14	4.50	7.16	15.3	516	849	342	395	n/s	51.0	0.02	130	4.50	0.30	14.0
CTCO2-2	Fluid ex core	501	0.04	4.50	10.5	22.4	1249	826	1853	870	95.2	30.0	0.02	452	4.50	0.30	1.50
CTCO2-3	Fluid ex core	645	0.04	4.50	6.56	14.0	845	209	2923	3.00	37.5	12.0	0.02	431	51.0	0.30	1.50
CTCO2-4	Fluid ex core	788	0.04	4.50	5.04	10.8	672	113	2242	3.00	37.5	6.00	0.02	434	27.0	0.30	1.50
CTCO2-5	Fluid ex core	961	0.04	4.50	4.18	8.94	559	76.0	1890	9.00	37.5	6.00	0.02	410	4.50	0.30	1.50
CTCO2-6	Fluid ex core	1125	0.04	4.50	3.48	7.44	485	60.0	1685	11.0	37.5	6.00	0.02	330	4.50	0.30	1.50
CTCO2-7	Fluid ex core	1292	0.04	4.50	3.25	6.95	483	56.0	1760	3.00	37.5	6.00	0.02	130	4.50	0.30	1.50
CTCO2-8	Fluid ex core	1462	0.04	4.50	2.82	6.03	452	52.0	1640	3.00	37.5	6.00	0.02	130	4.50	0.30	1.50
CTCO2-9	Fluid ex core	1630	0.04	4.50	2.38	5.09	408	44.0	1478	3.00	37.5	6.00	0.02	130	4.50	0.30	1.50
CTCO2-10	Fluid ex core	1798	0.04	4.50	2.29	4.90	403	42.0	1478	3.00	37.5	6.00	0.02	130	4.50	0.30	1.50
CTCO2-11	Fluid ex core	1965	0.04	4.50	2.26	4.83	417	46.0	1524	3.00	37.5	6.00	0.02	130	4.50	0.30	1.50
CTCO2-12	Fluid ex core	2132	0.04	4.50	2.02	4.32	377	42.0	1410	3.00	37.5	6.00	0.02	130	4.50	5.20	1.50
Starting fluid		0.00	0.04	4.50	0.07	0.15	0.50	2.00	1.00	3.00	n/s	6.00	0.02	130	4.50	0.30	1.50

Sample	Sample description	Total time	Cr	Co	Ni	Cu	Zn	Ga	As	Se	Rb	Y	Zr	Nb	Mo	Ag	Cd
			µg l^{-1}	µg l^{-1}	µg l^{-1}	µg l^{-1}	µg l^{-1}	µg l^{-1}	µg l^{-1}	µg l^{-1}	µg l^{-1}	µg l^{-1}	µg l^{-1}	µg l^{-1}	µg l^{-1}	µg l^{-1}	µg l^{-1}
CTCO2-1	Fluid ex core	355	5.60	57.2	610	163	30.0	1.00	43.0	2.50	181	0.02	0.30	0.30	100	0.62	1.06
CTCO2-2	Fluid ex core	501	1.90	134	2323	39.9	82.0	1.00	3.70	2.30	139	0.02	0.30	0.30	26.0	0.13	4.26
CTCO2-3	Fluid ex core	645	0.25	172	5322	2.4	35.0	1.00	1.70	1.80	65.9	0.02	0.30	0.30	18.0	0.04	1.19
CTCO2-4	Fluid ex core	788	0.25	176	4754	2.1	26.0	1.00	1.60	2.30	46.3	0.02	0.30	0.30	18.0	0.04	0.25
CTCO2-5	Fluid ex core	961	0.25	173	3969	1.0	28.0	1.00	1.30	1.50	35.5	0.02	0.30	0.30	18.0	0.04	0.10
CTCO2-6	Fluid ex core	1125	0.50	158	3249	0.70	11.0	1.00	1.20	1.20	28.0	0.02	0.30	0.30	16.0	0.04	0.13
CTCO2-7	Fluid ex core	1292	0.60	160	3378	1.9	10.0	1.00	1.60	0.45	25.5	0.02	0.30	0.30	13.0	0.04	0.09
CTCO2-8	Fluid ex core	1462	0.70	134	3298	1.4	6.0	1.00	1.50	1.00	21.5	0.02	0.30	0.30	13.0	0.04	0.04
CTCO2-9	Fluid ex core	1630	0.70	95.3	2890	1.1	5.0	1.00	1.50	0.45	17.6	0.02	0.30	0.30	12.0	0.04	0.04
CTCO2-10	Fluid ex core	1798	0.90	78.2	2866	1.4	8.0	1.00	1.30	0.45	16.1	0.02	0.30	0.30	13.0	0.04	0.09
CTCO2-11	Fluid ex core	1965	1.00	66.8	2769	1.4	5.0	1.00	1.80	0.45	15.4	0.02	0.30	0.30	14.0	0.04	0.04
CTCO2-12	Fluid ex core	2132	1.00	52.5	2490	1.1	4.0	1.00	1.80	0.45	13.6	0.02	0.30	0.30	13.0	0.04	0.18
Starting fluid		0.00	0.25	0.04	0.30	5.2	14.0	1.00	14.0	2.90	3.06	0.02	0.30	0.30	1.00	0.04	0.07

Sample	Sample description	Total time	Sn	Sb	Cs	La	Ce	Pr	Nd	Sm	Eu	Gd	Tb	Dy	Ho	Er	Tm
			µg l^{-1}	µg l^{-1}	µg l^{-1}	µg l^{-1}	µg l^{-1}	µg l^{-1}	µg l^{-1}	µg l^{-1}	µg l^{-1}	µg l^{-1}	µg l^{-1}	µg l^{-1}	µg l^{-1}	µg l^{-1}	µg l^{-1}
CTCO2-1	Fluid ex core	355	0.05	1.62	5.92	0.01	0.02	0.02	1.00	0.02	0.01	0.012	0.004	0.01	0.004	0.03	0.004
CTCO2-2	Fluid ex core	501	0.05	1.18	5.68	0.01	0.02	0.02	1.00	0.02	0.01	0.004	0.004	0.01	0.004	0.03	0.004
CTCO2-3	Fluid ex core	645	0.05	0.59	3.61	0.01	0.02	0.02	1.00	0.02	0.01	0.004	0.004	0.01	0.004	0.03	0.004
CTCO2-4	Fluid ex core	788	0.05	0.32	3.04	0.01	0.02	0.02	1.00	0.02	0.01	0.004	0.004	0.01	0.004	0.03	0.004
CTCO2-5	Fluid ex core	961	0.05	0.16	2.52	0.01	0.02	0.02	1.00	0.02	0.01	0.008	0.004	0.01	0.004	0.03	0.004
CTCO2-6	Fluid ex core	1125	0.05	0.10	2.14	0.01	0.02	0.02	1.00	0.02	0.01	0.004	0.004	0.01	0.004	0.03	0.004
CTCO2-7	Fluid ex core	1292	0.05	0.10	2.02	0.01	0.02	0.02	1.00	0.02	0.01	0.004	0.004	0.01	0.004	0.03	0.004
CTCO2-8	Fluid ex core	1462	0.05	0.09	1.69	0.01	0.02	0.02	1.00	0.02	0.01	0.004	0.004	0.01	0.004	0.03	0.004
CTCO2-9	Fluid ex core	1630	0.05	0.05	1.34	0.01	0.02	0.02	1.00	0.02	0.01	0.004	0.004	0.01	0.004	0.03	0.004
CTCO2-10	Fluid ex core	1798	0.05	0.05	1.20	0.01	0.02	0.02	1.00	0.02	0.01	0.004	0.004	0.01	0.004	0.03	0.004
CTCO2-11	Fluid ex core	1965	0.05	0.05	1.16	0.01	0.02	0.02	1.00	0.02	0.01	0.004	0.004	0.01	0.004	0.03	0.004
CTCO2-12	Fluid ex core	2132	0.05	0.05	1.03	0.01	0.02	0.02	1.00	0.02	0.01	0.004	0.004	0.01	0.004	0.03	0.004
Starting fluid		0.00	0.05	0.05	0.26	0.01	0.02	0.02	1.00	0.02	0.01	0.004	0.004	0.01	0.004	0.03	0.004

Sample	Sample description	Total time	Yb	Lu	Hf	Ta	W	Tl	Pb	Th	U
			µg l^{-1}	µg l^{-1}	µg l^{-1}	µg l^{-1}	µg l^{-1}	µg l^{-1}	µg l^{-1}	µg l^{-1}	µg l^{-1}
CTCO2-1	Fluid ex core	355	0.004	0.004	0.10	0.05	118	0.95	0.10	0.25	3.92
CTCO2-2	Fluid ex core	501	0.004	0.004	0.10	0.05	5.90	0.78	0.10	0.25	7.62
CTCO2-3	Fluid ex core	645	0.004	0.004	0.10	0.05	0.20	0.16	0.10	0.25	2.00
CTCO2-4	Fluid ex core	788	0.004	0.004	0.10	0.05	0.20	0.02	0.10	0.25	1.76
CTCO2-5	Fluid ex core	961	0.004	0.004	0.10	0.05	0.20	0.02	0.10	0.25	1.66
CTCO2-6	Fluid ex core	1125	0.004	0.004	0.10	0.05	0.20	0.02	0.10	0.25	1.41
CTCO2-7	Fluid ex core	1292	0.004	0.004	0.10	0.05	0.20	0.02	0.10	0.25	1.23
CTCO2-8	Fluid ex core	1462	0.004	0.004	0.10	0.05	0.20	0.02	0.10	0.25	1.07
CTCO2-9	Fluid ex core	1630	0.004	0.004	0.10	0.05	0.20	0.02	0.10	0.25	0.95
CTCO2-10	Fluid ex core	1798	0.011	0.004	0.10	0.05	0.20	0.02	0.10	0.25	0.89
CTCO2-11	Fluid ex core	1965	0.004	0.004	0.10	0.05	0.20	0.02	0.10	0.25	0.84
CTCO2-12	Fluid ex core	2132	0.004	0.004	0.10	0.05	0.20	0.02	0.10	0.25	0.75
Starting fluid		0.00	0.004	0.004	0.10	0.05	0.20	0.02	0.10	0.25	0.04

References

British Geological Survey holds most of the references listed below, and copies may be obtained via the library service subject to copyright legislation (contact libuser@bgs.ac.uk for details). The library catalogue is available at: http://geolib.bgs.ac.uk.

BEAUBIEN, S E., KRUEGER. M., CIOTOLI, G., COOMBS, P., DICTOR, M C., LOMBARDI, S., PEARCE, J M. AND WEST, J M. 2008. The impact of naturally occurring CO_2 gas vent on the shallow ecosystem and soil chemistry of a Mediterranean pasture (Latera, Italy). *Int. J. Greenhouse Gas Control*, 2, 373-387.

COOMBS, P., WAGNER, D., BATEMAN, K., HARRISON, H., MILODOWSKI, A E., NOY, D. AND WEST, J M. 2010. The role of biofilms in subsurface transport processes. *Quarterly Journal of Engineering Geology and Hydrogeology*, 43, 131-139.

D'HONDT, S., RUTHERFORD, S. AND SPIVACK, A J. 2002. Metabolic activity of subsurface life in deep-sea sediments. *Science*, 295, 2067-2070.

EHRLICH, H L. 1999. Microbes as geologic agents: their role in mineral formation. *Geomicrobiology Journal*, 16, 135-153.

HARRISON, H., WEST, J M., BATEMAN, K., CAVE, M., COOMBS, P., HARRINGTON, J., LACINSKA, A., MILODOWSKI, A E., TURNER, G H. AND WAGNER, D. 2009 Microbial effects on transport processes (BioTran) – Anaerobic flow-through Experiments using crushed Diorite and *Pseudomonas aeruginosa* (April 2008 – March 2009). *British Geological Survey Open Report OR/09/033.*

HARRISON, H., WAGNER, D., YOSHIKAWA, H., WEST, J. M. MILODOWSKI, A.E., SASAKI, Y., TURNER, G., LACINSKA, A., HOLYOAKE, S., HARRINGTON, J., NOY, D., COOMBS, P., BATEMAN, K. AND AOKI, K. 2011. Microbiological influences on fracture surfaces of intact mudstone and the implications for geological disposal of radioactive waste. *Mineralogical Magazine*, 75, pp 2449-2466. doi: 10.1180/minmag.2011.075.4.2449.

HILLIER, S., SUZUKI, K. AND COTTER-HOWELLS, J. 2001. Quantitative determination of cerussite (Lead Carbonate) by X-Ray Diffraction and inferences for lead speciation and transport in stream sediments from a former lead mining area of Scotland. *Applied Geochemistry*, 16, 597-608.

HOBBIE, J E., DALEY, R J. AND JASPER, S. 1977. Use of nucleopore filters for counting bacteria by fluorescent microscopy. *Applied and Environmental Microbiology*, 33, 1225-1228.

JASS, J. AND LAPPIN-SCOTT, H M. 1992. Practical course on biofilm formation using the modified Robbins Device. University of Exeter.

KHARAKA, Y K., COLE, D R., HOVORKA, S D., GUNTER, W D., KNAUSS, K G. AND FREIFELD, B M. 2006. Gas-water-rock interactions in Frio Formation following CO_2 injection: Implications for the storage of greenhouse gases in sedimentary basins. *Geology*, 34 (7), 577-580.

KRÜGER, M., WEST, J M., FRERICHS, J., OPPERMANN, B., DICTOR, M-C., JOULIAN, C., JONES, D., COOMBS, P., GREEN, K., PEARCE, J., MAY, F. AND MOELLER, I. 2009. Ecosystem effects of elevated CO_2 concentrations on microbial populations at a terrestrial CO_2 vent at Laacher See, Germany. *Energy Procedia*, 1, 1933-1939.

KRÜGER, M M., JONES, D., FRERICHS, J., OPPERMANN, B I., WEST. J M., COOMBS, P., GREEN, K., BARLOW, T., LISTER, B., STUTT, M. AND MÖLLER, I. 2011. Effects of elevated CO_2 concentrations on the vegetation and microbial populations at a terrestrial CO_2 vent at Laacher See, Germany. *International J. Greenhouse Gas Control*, 5, 1093-1098. doi. 10.1016/j.iggc.2011.05.002.

LIN, L-H., WANG, P-L., RUMBLE, D., LIPPMANN-PIPKE, J., BOICE, E., PRATT, L M., SHERWOOD LOLLAR, B., BRODIE, E L., HAZEN, T C., ANDERSEN, G L., DESANTIS, T Z., MOSER, D P., KERSHAW, D. AND ONSTOTT, T C. 2006. Long-term sustainability of a high-energy, low-diversity crustal biome. *Science*, 314, 479-482.

MAUL, P R., BEAUBIEN, S E., BOND, A E., LIMER, L M C., LOMBARDI, S., PEARCE, J., THORNE, M. AND WEST, J M. 2009. Modelling the fate of carbon dioxide in the near-surface environment at the Latera natural analogue site. *Energy Procedia*, 1, 1879-1885.

MILODOWSKI, A E., WEST, J M., PEARCE, J M., HYSLOP, E K., BASHAM, I R. AND HOOKER, P J. 1990. Uranium-mineralised microorganisms associated with uraniferous hydrocarbons in southwest Scotland. *Nature*, 347, 465-467.

MILODOWSKI, A E AND RUSHTON, J C. 2008. Mineralogical and porosity characterisation of potential aquifer and seal units for carbon capture and storage methodologies for the CASSEM project. *British Geological Survey Research Report, CR/08/153.*

MITCHELL, A C., PHILLIPS, A J., HIEBERT, R., GERLACH, R., SPANGLER, L H. AND CUNNINGHAM, A B. 2009. Biofilm enhanced geologic sequestration of supercritical CO_2. *International Journal of Greenhouse Gas Control*, 3, 90-99.

MOROZOVA, D., WANDREY, M., ALWAI, M., ZIMMER, M. AND VIETH, A. 2010. Monitoring of the microbial community composition in saline aquifers during CO_2 storage by fluorescence in situ hybridisation. *International Journal of Greenhouse Gas Control*, 4 (6) 981-989 (doi. 10.1016/j/ojggc,2009.11.014).

SNYDER, R L. AND BISH D L. 1989. *Quantitative Analysis* (Chapter 5)., In: Bish, D L., Post, J E. (Eds), Modern power diffraction. *Mineralogical Society of America Reviews in Mineralogy*, 20, 101-144.

TUCK, V A., EDYVEAN, R G J., WEST, J M., BATEMAN, K., COOMBS, P., MILODOWSKI, A E. AND MCKERVEY, J A. 2006. Biologically induced clay formation in subsurface granitic environments. *Journal of Geochemical Exploration 90*, 123-133.

VAUGHAN, D J., WOGELIUS, R., BOULT S. AND MERRIFIELD, C. 2001. Quantifying the effects of biofilm growth on hydraulic properties and on sorption equilibrium microscopic to macroscopic measurements. *Progress summary 02/01 – 11/01 Williamson Research Centre, University of Manchester*.

WEST, J M. AND CHILTON, P J. 1997. Aquifers as environments for microbiological activity. *Quarterly Journal of Engineering Geology* 30, 147-154.

WEST, J M., PEARCE, J., BENTHAM, M., ROCHELLE, C., MAUL, P. AND LOMBARDI, S. 2006. Environmental issues, and the geological storage of CO_2 – a European perspective. 8th International Conference on Greenhouse Gas Control Technologies. Trondheim, Norway, June 2006. Elsevier.

WEST, J M., MCKINLEY, I G., PALUMBO-ROE, B. AND ROCHELLE, C A. 2011. Potential impact of CO_2 storage on subsurface microbial ecosystems and implication for groundwater quality. *Energy Procedia*, 4, 3163-3170. doi:10.1016/j.egypro.2011.02.231.

WEST, J M., BATEMAN, K., COOMBS, P., HARRISON, H M., MILODOWSKI, A E., RUSHTON, J., TURNER, G., WAGNER, D. AND WRAGG, J. 2011. Microbiological effects on transport processes (BioTran) – Data production from column experiments containing Sherwood Sandstone (October 2010 - July 2011). British Geological Survey Open Report, 11/058.

WRAGG, J., HARRISON, H., WEST, J M. AND YOSHIKAWA, H. 2012. Comparison of microbiological influences on the transport properties of intact mudstone and sandstone and its relevance to the geological disposal of radioactive waste. *Mineralogical Magazine* 76, 3251-3259.